ATMOSPHERIC ELECTRICITY

NEWSLETTER

Vol.36 2025
No.1 May

Artistic view of a NASA plane flying over gamma ray-glowing clouds in the Caribbean during the July 2023 flight campaign.

Photo by UiB/Mount Visual

Cover Story :

A view from a retrofitted spy plane soaring at 20 kilometers up revealed storms glowing and flickering in gamma rays, high-energy light invisible to the eye. Ten flights with the plane, NASA' s ER-2 aircraft, captured the shimmer of gamma-ray outbursts over a variety of timescales and intensities, suggesting that the emissions are more complex and more common than previously thought. And the study unveiled a brand-new type of gamma-ray blast the researchers named a flickering gamma-ray flash.

More details refer to N. Østgaard et al. Flickering gamma-ray flashes, the missing link between gamma glows and TGFs. Nature. 634, Oct. 3, 2024, p. 53.
M. Marisaldi et al. Highly dynamic gamma-ray emissions are common in tropical thunderclouds. Nature. 634, Oct. 3, 2024, p. 57.
I. Bjørge-Engeland et al. Evidence of a new population of weak terrestrial gamma-ray flashes observed from aircraft altitude. Geophysical Research Letters. 51, Sep. 7, 2024, e2024GL110395.

ICAE
IAMAS IUGG
https://www.iamas.org/icae/

18th International Conference on Atmospheric Electricity

Barcelona, July 13-17, 2026

https://icae2026.upc.edu

Dear Friends and Colleagues,

We are delighted to invite you the 18th International Conference on Atmospheric Electricity (ICAE 2026), which will be held in the colorful city of Barcelona, Spain. The International Conference on Atmospheric Electricity is the world's largest event dedicated to advancing the science of atmospheric electricity. ICAE 2026 provides an opportunity for researchers from all over the world to present the latest discoveries, exchange ideas, and the most important: learn, interact with your colleagues and make new friends.

This is the first time that ICAE 2026 lands in Spain. Our tradition in modern atmospheric electricity is dated at the beginning of XX century (1904) with measurements of atmospheric potential gradient, ions and air conductivity, and radio detection of lightning. After more than 100 years of tradition in atmospheric electricity, we are proud to host the ICAE 2026 in Spain.

The conference will be host at the Universitat Politecnica de Catalunya (Diagonal Campus) in Barcelona from July 13 to17, 2026.

Call for Abstracts

Topics include:

- Lightning Physics
- Lightning and Meteorology
- Meteorological Applications of Lightning Data
- Energetic Radiation from Lightning and Thunderstorms

- Thunderstorm Electrification and Microphysics
- Lightning Effects on the Middle and Upper Atmosphere
- Lightning Climatology and Chemical Effects
- Lightning and Thunderstorm Detection Technologies
- Space-based Lightning Detection
- Lightning Effects, Hazards and Mitigation
- Fair Weather and Atmospheric Ions
- Global Electric Circuit
- Planetary Lightning
- Ball lightning
- Climate Change and Atmospheric Electricity
- Artificial Intelligence (including Machine Learning) in Atmospheric Electricity.
- Related Topics

Abstract submission is now open!

Submission deadline: October 31, 2025

Notification of acceptance and oral/poster presentation: January 31, 2026

Co-Chairs:

Eric Defer (LAERO) Joan Montanyà (UPC) Nicolau Pineda (SMC)

Serge Soula (LAERO) Oscar van der Velde (UPC)

Contact:

icae2026@event.upc.edu

Final Report of the Task Team on Lightning Observations for Climate Applications (TT-LOCA)

Contributor: Steven Goodman, NOAA/NASA GOES-R Program Senior Scientist, Emeritus, tgabama@gmail.com

The Atmospheric Observation Panel for Climate (AOPC) agreed during AOPC-22 (Exeter, UK, March 2017, (GCOS, 2017)) on the creation of a dedicated Task Team on Lightning Observations

for Climate Applications (TT-LOCA). The WMO published the report GCOS-227 on the initial findings and recommendations of the task team in 2019 (WMO, 2019). To allow on-going work to continue, some unfinished tasks to be completed, and allowing for the impacts of COVID-19, the Task Team tenure was extended. Interim progress reports were submitted to the AOPC and annual reports on climate for lightning were published in the American Meteorological Society Special Supplements on the State of the Climate (Blunden and Boyer, 2022; 2024; Blunden, J., T. Boyer, and E. Bartow-Gillies, 2023). The State of the Climate summaries include the planned lightning ECV quantities and anomalies for the recent La Niña and El Niño events, observed by satellite lightning imagers and by ground-based global networks. This final report summarizes the work done by TT-LOCA and covers key aspects of lightning observations for climate applications. The report also describes the status of observations and data stewardship, discusses gaps and open research questions and provides recommendations for monitoring specifications for lightning, including metadata requirements.

Blunden, J. and T. Boyer, Eds., 2022: "State of the Climate in 2021". Sidebar 2.1: Lightning— M. Füllekrug, E. Williams, C. Price, S. Goodman, R. Holzworth, K. Virts, and D. Buechler, Bull. Amer. Meteor. Soc., 103 (8), Si–S465, https://doi.org/10.1175/2022BAMSStateoftheClimate.1.

Blunden, J., T. Boyer, and E. Bartow-Gillies, Eds., 2023: "State of the Climate in 2022". 4. LIGHTNING, M. Füllekrug, E. Williams, C. Price, S. Goodman, R. Holzworth, K. Virts, D. Buechler, T. Lang, and Y. Liu, Bull. Amer. Meteor. Soc., 104 (9), Si–S501 https://doi.org/10.1175/2023BAMSStateoftheClimate.1.

Blunden, J. and T. Boyer, Eds., 2024: "State of the Climate in 2023". 4. THUNDER HOURS —M. Füllekrug, E. Williams, C. Price, S. Goodman, R. Holzworth, J. Lapierre, E. DiGangi, R. Said, M. McCarthy, K. Virts, A. M. Grimm, and Y. Liu, Bull. Amer. Meteor. Soc., 105 (8), Si–S483 https://doi.org/10.1175/2024BAMSStateoftheClimate.1.

WMO, 2019. GCOS-227 Lightning for Climate: A Study by the Task Team on Lightning Observation for Climate Applications (TT-LOCA) of the Atmospheric Observation Panel for Climate (AOPC), 56 pp.

WMO, 2025: Final Report of the Task Team on Lightning Observations for Climate Applications (TT-LOCA), 2024, GCOS-267, 19 pp. https://library.wmo.int/viewer/69477/download?file=GCOS-267-TT-LOCA-Final-Report_en.pdf&type=pdf&navigator=1.

Richard E. Orville

It will surely sadden many members of the atmospheric electricity community to learn that Richard E. Orville passed away on May 20th, 2024, in College Station, Texas. Dick made critical contributions in many areas of lightning research over a lengthy and distinguished career. He also had many collaborators in the U.S. and abroad who genuinely enjoyed working with him. A formal obituary for Dick will appear in the June issue of the Bulletin of the American Meteorological Society. Those wishing to send expressions of sympathy and condolence can do so via e-mail to Barbara Orville (b_orville@yahoo.com).

Vincent P. Idone, Ph.D.
Associate Professor Emeritus
Dept. of Atmospheric and Environmental Sciences
U-ALBANY ETEC Building - Harriman Campus
University at Albany, SUNY
1220 Washington Ave., Room 496
Albany, NY 12226
Cell: (518) 860-7918
E-mail: vidone@albany.edu

African Centres for Lightning and Education Network (ACLENet)

ACLENet has been serving Africa for over a decade and is broadening its focus for the decade ahead.

1. Rebranding

a. New NAME -- While retaining ACLENet, the name has changed from African Centres for Lightning and Electromagnetics Network to African Centres for Lightning Education Network to emphasize a new focus.

b. New logo – see above

c. New website – ACLENet.org

d. Soon a reformatted newsletter

2. Broadened Focus

For the first ten years, ACLENet concentrated on the physical protection of schools, students, and teachers from lightning injury as well as research and investigation of these injuries. Its focus for the next decade will concentrate much more on education including behavioral lightning safety education at schools and in communities and work with the media that will enable people to decrease their risk of injury.

3. Leadership

ACLENet has recruited and is orienting an expanded Board of Directors that includes members from seven countries who have broad experience in nonprofits as well as lightning.

Since our last report, both educational programs, lightning clubs at schools, and repairs and enhancements of lightning protection systems at many of the nine schools we have protected have been accomplished.

Additionally, two members of ACLENet's Board, Mary Ann Cooper (USA), and Ken Nixon (South Africa, UWits) will be traveling to Uganda to attend the International Lightning Safety Day (28 June) commemoration of when 18 children were killed and another 38 hospitalized from a single lightning strike to their school in 2011. The Honorable Hilary Onek, Minister of Disaster Preparedness and Refugees, long a mentor of ACLENet, has agreed to be Guest of Honor at this event where over 2000 people are expected to attend.

CMA Key Laboratory of Lightning, State Key Laboratory of Severe Weather, Chinese Academy of Meteorological Sciences, Beijing, China

Higher proportion of high-energy lightning strokes in global high-altitude areas. By examining proportions of high-energy strokes from the World Wide Lightning Location Network (WWLLN) between 60°S and 60°N, and high-radiance events from the Lightning Imaging Sensor (LIS) between 38°N and 38°S, along with the average energies of WWLLN strokes and LIS events with specific thresholds, we discovered significantly higher proportions of high-energy lightning strokes and greater average stroke energies over high-altitude terrains, a phenomenon not previously reported. These highlands include the Tibetan Plateau, Mongolian Plateau, Iranian and Anatolian Plateaus, South African Plateau, mountain regions in western North America, and Andes Mountains. In terms of both proportion and average energy, high-energy WWLLN strokes show a stronger correlation with highlands than high-energy LIS events. Considering the different observation modes of WWLLN and LIS, this may suggest a stronger connection between highlands and high-energy lightning strokes occurring beneath and in the lower parts of thunderstorms.

Striking distance characteristics of lightning flashes striking at and below the top of the Canton Tower. When lightning bypasses the lightning rod at the top of a building and strikes the side of the protected object, it forms a so-called side-strike lightning. Due to side-strike lightning, installing lightning rods on the top of high buildings still cannot achieve 100% lightning interception efficiency. The side-strike lightning may cause electrical current to pass through the building's metal doors, windows, or electrical circuits and enter the interior, posing a threat to internal personnel and electronic and electrical equipment. At present, there is little research on side-strike lightning and even less research on the characteristics of the striking distance (SD) of side-strike lightning, mainly because the probability of side-strike lightning occurring is low. A total of 19 lightning flashes observed by high-speed video cameras were selected for analyzing the two-dimensional SD before the first return stroke of downward negative cloud-to-ground lightning flashes striking at the Canton Tower (600 m high). Among them, 13 lightning flashes directly struck at the top of the Canton Tower, and six lightning flashes struck at positions 8 to 146 m below the top of the Canton Tower. It was found that the higher the lightning strike position at the Canton Tower, the longer the SD,

and the closer it is to the top of the tower, the faster the SD increases. On average, the first return stroke peak current for the lightning striking at the top of the Canton Tower was 86 kA, while the average value for side-strike lightning was less than 33 kA, with only about 38% of the former (Figure 1).

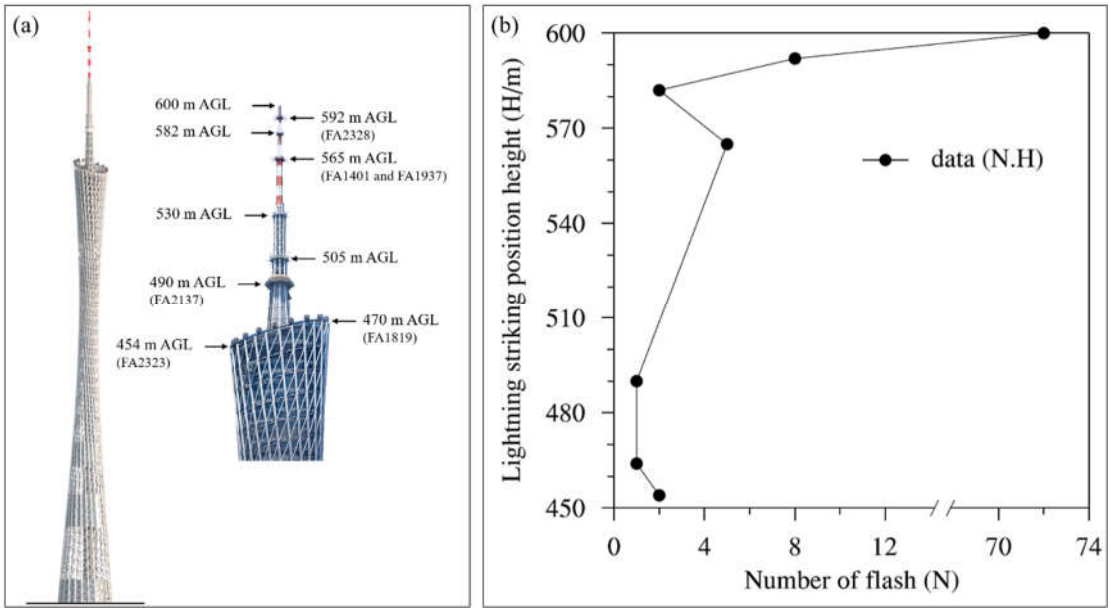

Figure 1. (a) Details of Canton Tower and its upper part, and (b) The number of downward negative CG lightning flashes and their corresponding strike position height on the 600-m high Canton Tower. At different positions on the antenna mast, there are several circular platforms with horizontally outward lightning protection devices on the periphery of the platforms.

Thunderstorms with extreme lightning activity in China: climatology, synoptic patterns, and convective parameters. Intense convection is often accompanied by high-frequency lightning and is highly prone to producing heavy rainfall, strong winds, hail, and tornadoes, frequently resulting in significant damage and loss of life. It is necessary to understand the mechanisms and meteorological conditions of intense convection. This study utilizes the Thunderstorm Feature Dataset from 2010–2018 to analyze the characteristics of thunderstorms with extreme lightning activity (TELAs), defined as thunderstorms whose lightning frequency ranks in the top 1%. Four regions with relatively high thunderstorm activity were selected for analysis: Northeast China (NEC), North China (NC), South China (SC), and the Tibetan Plateau (TP). In NEC, TELAs primarily occur just west of upper-level westerly troughs (UWT), including cold vortices. In NC, TELAs are mainly associated with UWT and subtropical highs (STH). In SC,

TELAs are related to frontal systems, easterly waves, tropical cyclones, and STH. In TP, TELAs are generated by TP vortices. Before the TELA process, vertically integrated moisture divergence (VIMD) and convective available potential energy (CAPE) show the most notable anomalies. Except for the TP, TELAs are typically located between centers of anomalies with positive and negative geopotential height (500 hPa) and near centers of anomalies with positive CAPE and negative VIMD, accompanied by notable increases in surface temperature and wind speed. These findings offer a valuable reference for the early warning and forecasting of intense convection.

Analysis of anomalous cloud-to-ground lightning in a Wuhan tornadic supercell on 14 May 2021. Data primarily from the China Lightning Detection Network and dual-polarization radars were analyzed to investigate the cloud-to-ground lightning activity and its relationship with the thunderstorm structure in a supercell in Wuhan, Hubei, China, on May 14, 2021. This storm produced an EF3-scale (Enhanced Fujita Scale) tornado and exhibited complex variations in cloud-to-ground lightning activity. The dominant polarity of cloud-to-ground lightning transitioned from negative to positive and back to negative, with each polarity reversal accompanied by a decrease in cloud-to-ground lightning frequency. During a period when positive cloud-to-ground flashes accounted for 92.7 % of all cloud-to-ground flashes, the mean peak current reached an extraordinary 96.1 kA, significantly higher than during other periods or for negative cloud-to-ground lightning throughout the thunderstorm's lifetime. The tornado occurred near the peak of positive cloud-to-ground lightning activity. Based on an analysis of the relationship between cloud-to-ground lightning activity and the dynamic and microphysical parameters derived from radar data, it is deduced that the storm's charge structure likely evolved through the following sequence: an initial normal tripolar structure with predominant negative cloud-to-ground lightning, transitioning to an inverted tripolar structure during the dominance of positive cloud-to-ground lightning, followed by an inverted dipolar structure with a temporary increase and predominance of negative cloud-to-ground frequency, and finally returning to a normal tripolar structure characterized by high-frequency, predominantly negative cloud-to-ground lightning. The high peak current of positive cloud-to-ground lightning may be attributed to increased charge density from intense convection and a strong environmental electric field, particularly at lower lightning initiation altitudes.

Evolution of charge structure in a thunderstorm over South China. South China is one of the most active regions for thunderstorms in China, yet, research on the charge structure of thunderstorms in this area remains limited. This study utilized lightning

data from the Guangdong Lightning Mapping Array and radar observations to examine the charge structure of a thunderstorm that occurred in South China on June 16, 2021. The thunderstorm's charge structure underwent transitions from a dipole in the early stage, a tripole during its mature stage, and back to a dipole in the dissipation period. The heights of the two charge regions in the initial dipolar charge structure increased rapidly. Throughout the storm, the lower positive charge region in the tripolar charge structure was involved in 11.8% of the total 1075 recorded flashes. The average distances between the high-density charge cores of the three charge regions were 2.8 km and 2.6 km from top to bottom. As the storm entered its dissipation stage, the upper positive charge region descended significantly more slowly than the larger particles, as indicated by the continuous decrease in radar reflectivity in this region. The dominant hydrometeors in the upper positive, middle negative, and lower positive charge regions were dry aggregated snow, graupel, and larger-size graupel, respectively, occupying approximately 81%, 67%, and 70% of the total volume in each region. Over the course of the three stages—when the lower positive charge region was initially uninvolved in discharges, became involved, and then ceased participation—the primary microphysical processes in the precipitation beneath the convective core were collisional breakup, size sorting, and collision-coalescence, respectively.

Gifu University, Japan

Observation of the first stepping process of three winter lightning discharges. Using three different lightning observation systems, we have observed the first stepping processes of three lightning discharges with unprecedented details. We show an example in Figure 1. We found that each of the first stepping processes contains a clear upward fast negative breakdown (FNB) corresponding to the preliminary breakdown (PB) pulse peak. Prior to the FNB from the lightning initiation, most sources are located in a fan-shape area, and the FNB grows from this area forming a channel with a length from 45 m to 120 m. During the period of about 100 microseconds immediately preceding the PB pulse, multiple 1 to 12 MHz radio bursts are located within or near the fan shape area. These radio bursts may indicate stem/space leaders. Eventually the FNB decayed and scattered in another fan shape area at the upper end of the channel. Based on these findings, we have proposed a complete picture of the first stepping process. This study has been published in GRL.

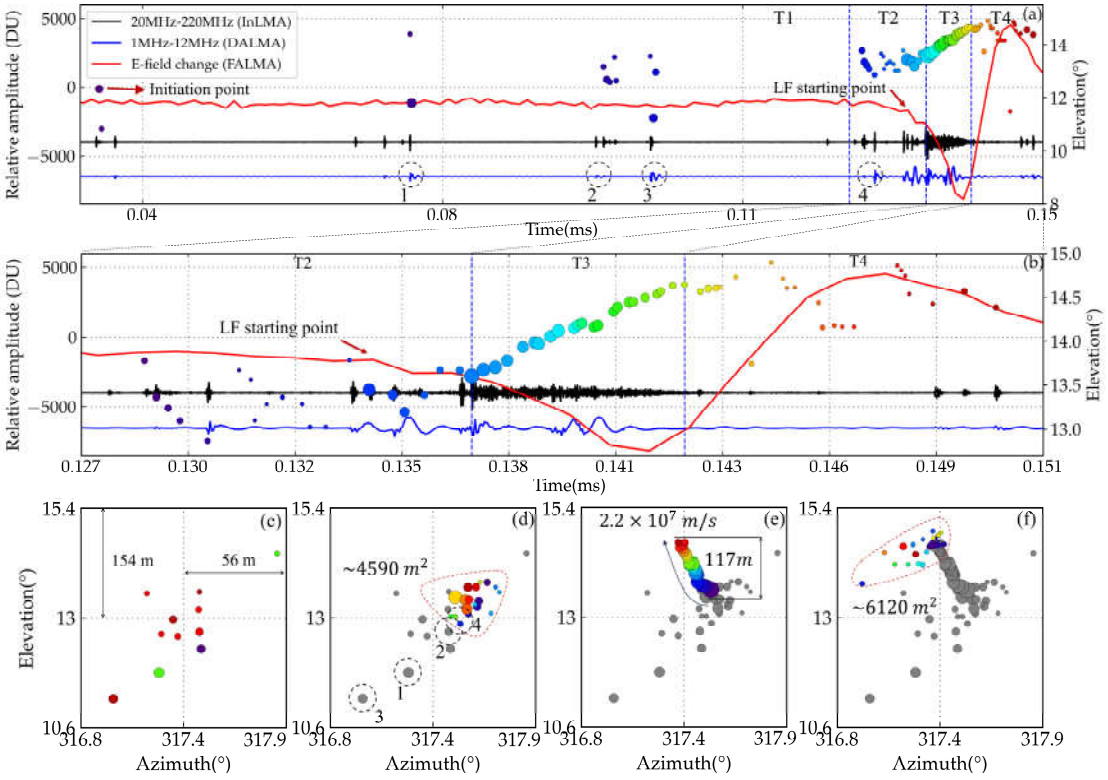

Figure 1. Enlarged view of the lightning initial process and first typical PB pulse. Panel (a) is divided into four stages, T1, T2, T3, and T4, corresponding to panels c, d, e, and f, respectively. The points color coded by time, and their size corresponds to the VHF amplitude. Panel (b) is an expansion of partial panel (a) for better viewing the process particularly during T3. Panel (c) is for the very initial stage. The discharge area in panel (d) is approximately 4590 m^2. The progression speed in panel (e) is 2.2 × 10^7m/s, with an extended distance of 117 m. The discharge area in panel (f) is approximately 6120 m^2.

Initiation Process of a Winter Cloud-to-Ground Lightning Flash. Lightning often originates deep within thunderclouds, making the lightning initiation research challenging. In this study, using a broadband (from 1 to 250 MHz) interferometer with high temporal-spatial resolution, we have observed the lightning initiation process of a winter cloud-to-ground lightning in Japan with great details. Figure 2 shows a detailed image of the lightning initiation. From Figures 2b-2f, we found that the lightning initiation involved multiple fast breakdowns behaving like a series of back (downward) and forth (upward) consecutive reflections in a constrained space near the main negative charge region of the lightning. We also found that some initial negative fast breakdowns could propagate with an unusually spread manner. We suggested that fast breakdowns with either reflecting features or spread manners could efficiently utilize the electrostatic energy in a local region with

strong electric field for driving subsequent streamers, and therefore may widely exist in lightning initiation processes. We also suggested that a lightning discharge may be usually triggered by a gust of wind. This study has been published in JGR: Atmospheres.

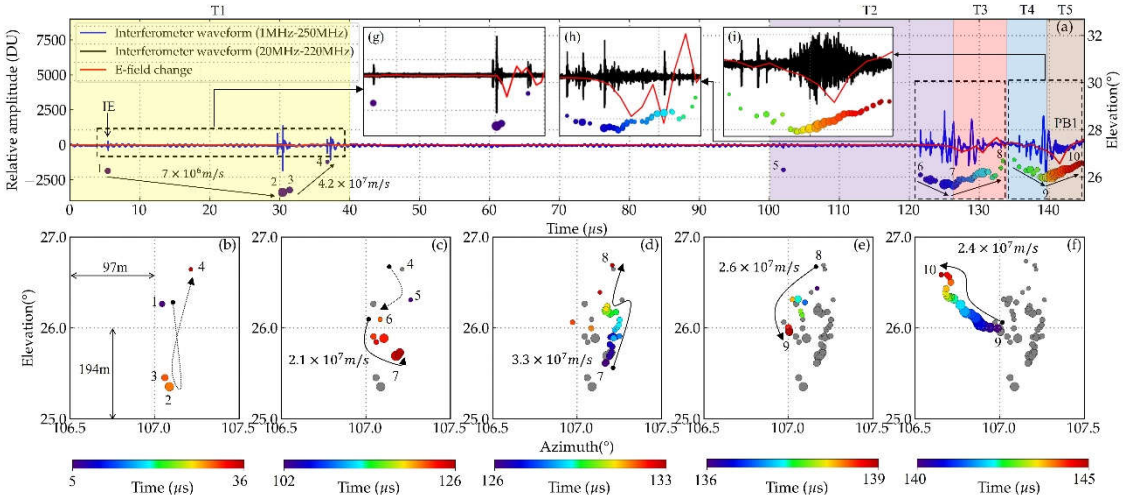

Figure 2. Enlarged view of the lightning initiation. In panel (a), the blue line is for the interferometer raw data and the red line is for the E-field change; the color dots coded in time are for the elevation of the 2D mapping versus time with their sizes indicating the corresponding VHF amplitudes, the blacklines in the "g," "h," and "i" boxes are for the interferometer data in the 20– 220 MHz frequency band. Points denoted from 1, 2, 3, 4, 5, 6, 7, 8, 9, and 10 are for reference. Panels (b), (c), (d), (e), and (f) corresponding to different time windows of T 1, T 2, T 3, T 4, and T 5 in panel (a), respectively. Gray dots are for points located previously, and arrows with dotted lines indicate the progression directions of the breakdowns. Also included are the mesh scales and the corresponding propagation speeds.

Preliminary Breakdown Process of Winter Positive Cloud-To-Ground Lightning and Its Relation to the Following First Return Stroke. We have studied the preliminary breakdown (PB) process and its relation to the following positive first return stroke (RS) for 60 winter positive cloud-to-ground (+CG) lightning flashes using their 3D mapping data by Discone Antenna Lightning Mapping Array in conjunction with the E-field change information by Fast Antenna Lightning Mapping Array. 31 (52%) PBs are found to propagate upward, 27 (45%) downward, and the remaining 2 (3%) with some initial progression direction reversal features. The winter +CG PBs can be characterized with an initiation height from 0.9 to 4.4 km, a propagation distance from 0.2 to 2.6 km, a propagation speed from 3.5×10^5 to 5.4×10^6 m/s without significant differences between upward and downward PBs. The time interval and the 2D displacement distance from the PB

initiation to the first RS range from 6.1 to 603.7 ms, from 0 to 39.2 km, respectively. We show the distribution of these six parameters in Figure 3. Return strokes with strongest intensities tend to have shorter intervals and 2D displacements between PB and RS. We also found some weak correlations between the PB characteristic parameters. All 60 +CGs involved multiple charge regions with opposite polarities and small separations. Finally, we have discussed our findings. This study has been published in JGR: Atmospheres.

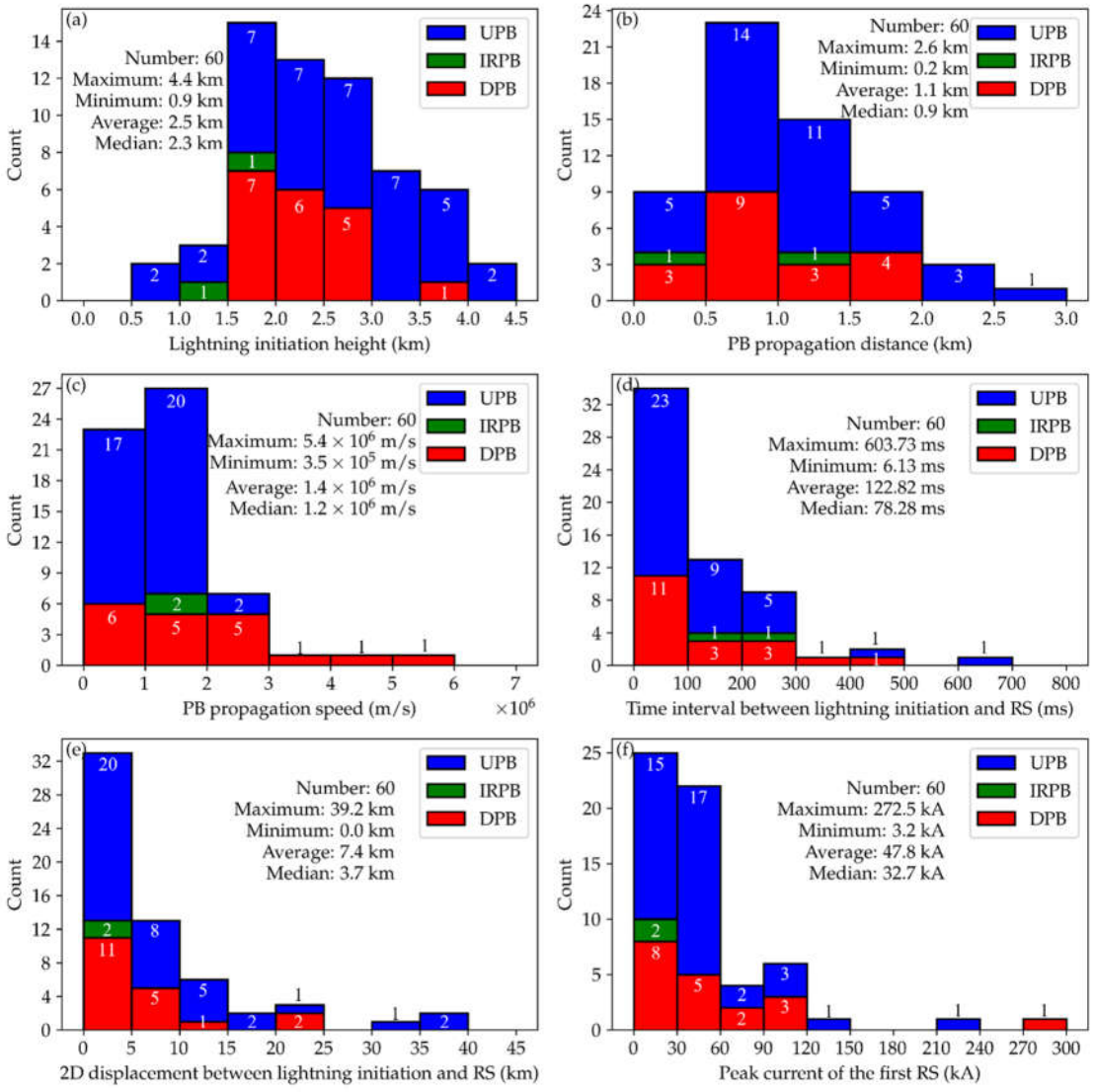

Figure 3. Statistical histograms for the six characteristic values measured with blue for UPB, red for DPB, and green for IRPB. In the blank area of each subplot, the number of statistics, maximum, minimum, average, and median values are shown. Numbers on each bar indicate the corresponding count. (a) Lightning initiation height. (b) PB propagation distance. (c) PB propagation speed. (d) Time interval between lightning initiation point and return stroke (RS). (e) 2D displacement between lightning initiation and RS. (f) Peak current of the first RS.

Energetic Compact Strokes in winter thunderstorms in Japan and their relationship with downward TGFs. In this study we report a special type of strong negative lightning stroke, termed energetic compact stroke (ECS), in winter thunderstorms in Japan, and provide strong evidence that ECSs are consistently associated with downward TGFs. Based on this relationship, we successfully identified three new downward TGFs by the observations of ECSs. Further, 12 out of 19 (63%) of downward TGFs analyzed in this paper were associated with ECSs, indicating that ECSs are the major source of downward TGFs in winter thunderstorms in Japan. These findings open up the possibility of remotely monitoring a large fraction of downward TGFs with simple lightning observations. Figure 4 shows FALMA waveforms of ten ECSs. We can see ECS waveforms are different from normal return strokes in several respects, so they were not recognized as CG strokes for many years. The yellow lines in Figure 4 indicate the onset of downward TGFs, and we can see that in most cases downward TGFs started right after the peak of the return stroke. This study has been published in GRL.

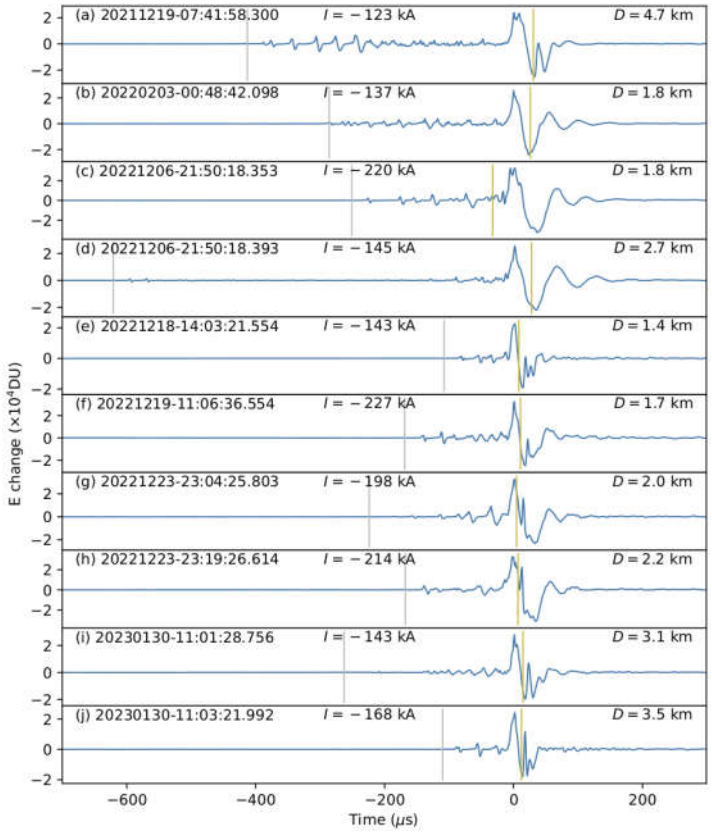

Figure 4. FALMA waveforms of ECSs coincident with TGFs. Vertical gray lines represent the first leader pulse (the start of the lightning flash). Yellow vertical lines represent the onset of TGFs. Values of *I* represent estimated peak currents of ECSs. Values of *D* represent distances from the ECS to the detector detecting the TGF.

HUN-REN Institute of Earth Physics and Space Science, Sopron, Hungary

Contributors: József Bór, Gabriella Sátori, Tamás Bozóki

Gabriella Sátori contributed to the paper titled "Reduction in Global Lightning Activity During the COVID Pandemic" with handling OTD/LIS satellite lightning data for different ENSO episodes (Liu et al., 2025).

Tamás Bozóki spent three months at the AGH University of Krakow (Poland) in the autumn of 2024, working together with Janusz Mlynarczyk on the automatic detection of lightning continuing currents using broadband ELF measurements. It seems that the complexity of ELF waveforms necessitates the development of a machine learning-based approach to tackle this problem. They also finalized a long-standing manuscript on the comparison of theoretical ELF spectra (5-50 Hz) produced by a simplified analytical and a full numerical (FDTD) model of Schumann resonances (SRs), which also considered SRs excited by lightning discharges with a continuing current. The study, which shows a high similarity between the output of the two models, is currently under review in JGR: Atmospheres (Bozóki et al., 2025).

In February 2025, a new online seminar series called "ELF Electromagnetic Waves and Ionospheric Physics Seminar" was launched in cooperation between the Krakow ELF group and the HUN-REN Institute of Earth Physics and Space Science, more details of which are available at the following link: https://www.oa.uj.edu.pl/elf/index/ELFseminar.htm.

International Lightning and TLE observation experiment 2025

Axiom Space's AX4 mission is expected to be launched this Summer. Lightning and transient luminous events (TLEs) in and above forecasted thunderstorm targets are to be recorded on video by the AX4 crew from the Cupola of the ISS. This will be the UHU experiment suggested jointly by researchers of the HUN-REN Institute of Earth Physics and Space Science, Hungary and RUNI University, Israel, József Bór and professor Yoav Yair,

respectively. The UHU experiment has been presented recently on the EGU25 General Assembly in Vienna, Austria (Bór et al., 2025). The contribution briefly reviews previous similar observation campaigns and highlights directions of research where such missions can yield significant new scientific results. Parallel to the UHU experiment, a world-wide ground-based observation campaign is planned to collect as much information about TLEs and their effects on the atmosphere as possible. Contribution of research institutions and citizen observers to this project is very welcome. Upon interest, please contact Bor.Jozsef@epss.hun-ren.hu.

Bór J, Y Yair, T Hegedüs, Z Jäger. 2025. UHU- another experiment to observe lightning and TLEs from the ISS. EGU General Assembly 2025, Vienna, Austria, 27 Apr–2 May 2025, EGU25-5994, https://doi.org/10.5194/egusphere-egu25-5994. Access at https://epss.hu/~jbor/Pub/Bor_et_al_2025_EGU_Poster.pdf.

Institute of Applied Physics, Russian Academy of Sciences, Nizhny Novgorod, Russia

A new understanding of seasonal variation of GEC. Seasonal variation of the ionospheric potential and the associated variability of surface measurements of the quasi-static electric field of the atmosphere is a question that still does not have an explicit answer. Back in 2007, Ralph Markson stated: «The annual variation of global geoelectric potential intensity is not known». Despite the large number of studies on the annual variation of GEC parameters, many questions remain unanswered. In a new study, new results on the character of the annual variation of the ionospheric potential are obtained on the basis of long-term changes in Antarctica, at Vostok station, a critical analysis of previous measurement data and on the basis of numerical modeling of more than 4 decades:

1. It is highly likely that there exists a stable annual cycle in the GEC intensity. For a number of reasons, this cycle is difficult to reliably determine from observations of atmospheric electrical parameters.

2. Measurements at the Vostok station in Antarctica predict the highest and lowest values of the diurnal mean GEC intensity during the Northern Hemisphere summer and winter, respectively.

3. The resulting annual variation of the GEC, being the sum of three clear patterns offsetting each other, is subtle and hard to simulate.

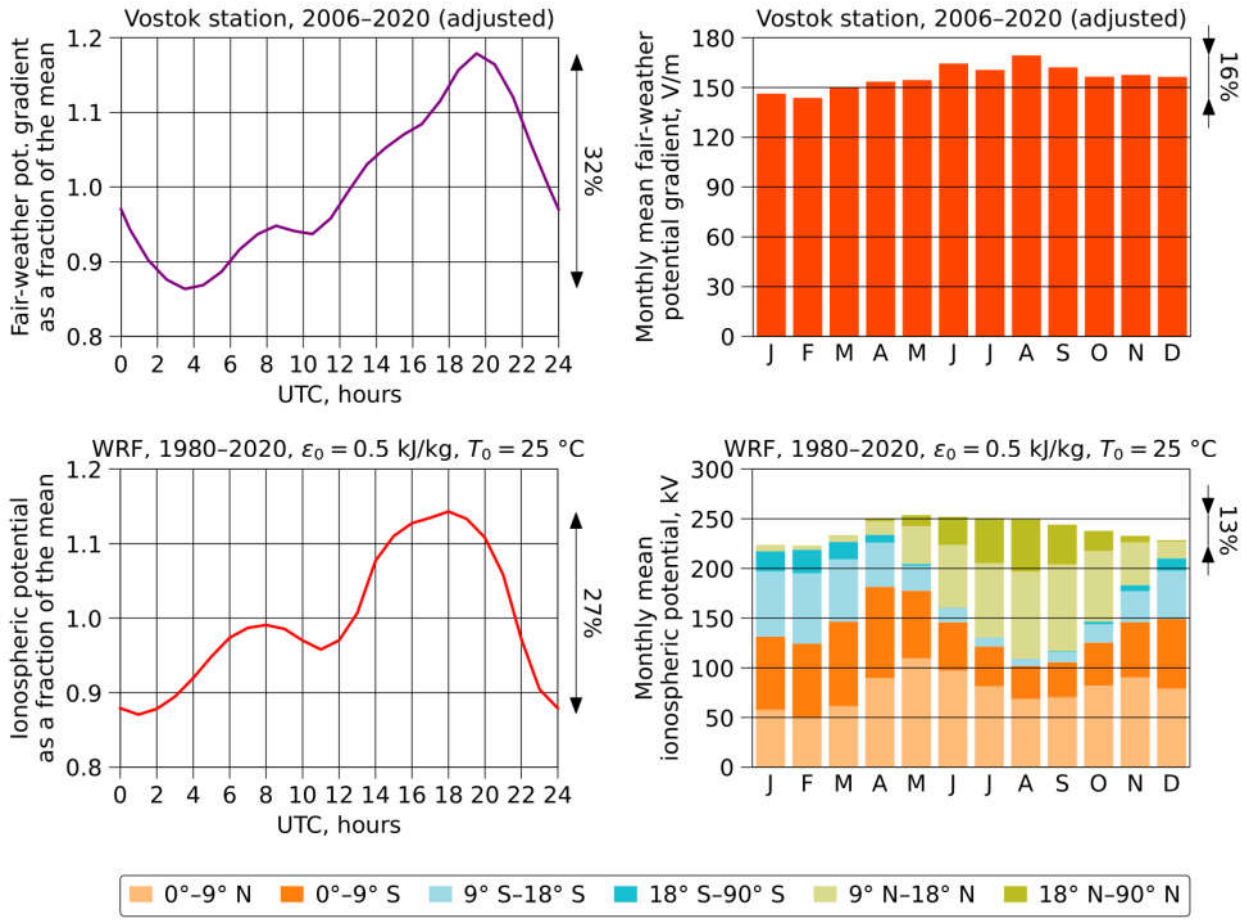

Figure 1. Character of the annual variation of the ionospheric potential on the basis of long-term changes in Antarctica, at Vostok station and numerical modeling.

Institute of Atmospheric Physics, Chinese Academy of Sciences (IAP, CAS), Beijing, China

Charge structure of an isolated thunderstorm on the Tibetan Plateau and the formation of bolt-from-the-blue lightning. By utilizing very high frequency (VHF) broadband interferometer lightning mapping technique, weather radar, and radio sounding, a thunderstorm process that produced two rare “bold-from-the-blue” (BFB) flashes was observed in the Lhasa area located in the central Plateau. The mechanism of the BFB flashes was revealed through accurate mapping of the discharge processes in high spatial and temporal resolution, and the corresponding charge structure characteristics inside the thunderstorm were also retrieved. At the initial stage of the thunderstorm, it exhibited a negative dipole charge structure with an upper negative and bottom positive

pattern, which is completely different from the evolution of charge structure in the thunderstorms over prominently lower altitude regions. When the thunderstorm developed into its mature stage, it exhibited a tripolar charge structure stacked with positive, negative, and positive charge regions from the top to bottom of the thunderstorm. These regions corresponded to environmental temperature zones below –30°C, from –30°C to –15°C, and above –10°C, respectively. The BFB flashes were associated with the upper dipole. The discharge originally initiated between the central negative and the upper positive charge region, with the positive leader developing downward to the lower negative charge region and the negative leader upward to the upper positive charge region. When the upward negative leader reached the upper positive charge region, it propagated horizontally and got out from the body of the small storm cell. The discharge ultimately became the BFB discharge process, spreading away from the cloud body into the clear sky area and striking the ground. The grounding points of the two BFB flashes were 3.6km and 3.8km from the precipitation edge of the storm, respectively. The horizontal scale of the thunderstorm cell was relatively small with positive charge regions in both the upper and lower parts of the cloud. The unbalanced upper dipole in the smaller storm body, where the upper positive charge region was weaker than the lower negative charge region, was the main reason for triggering the "bolt-from-the-blue" flashes. The evolution of the BFB thunderstorm is shown in Figure 1. (Qie et al., 2025)

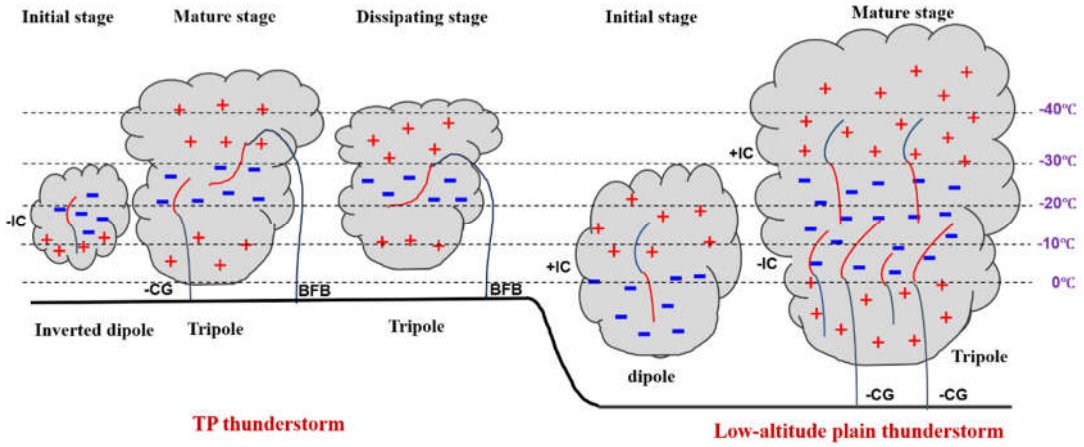

Figure 1. Schematic diagram of evolution of the thunderstorm charge structure and lightning discharges in central Tibetan Plateau and low altitude region at the same latitude. BFB stands for bolt-from-the-blue lightning. Red "+" for positive charge region, and blue "–" for negative region. Red curves represent for positive lightning channels, blue curves for negative channels, and black dash lines for environmental temperature.

Convective injection into stratospheric intrusions alters the tropopause chemical structure. The tropopause chemical structure (TCS) is influenced by stratosphere-troposphere exchange (STE) and plays a role in the Earth's climate. However, this role is still not fully understood in East Asia, where active STE and high anthropogenic emissions coexist. Using airborne measurements of trace gases, including O3, CO, and H2O, we reveal the variations in TCS during two consecutive cut-off lows (COLs), an important trigger of STE. We demonstrate the important roles of two-way STE and long-range transport processes in delivering natural and anthropogenic signatures in the TCS. The former COL case shows a normal pattern of TCS, consisting of stratospheric and tropospheric air and a mixture of them. The latter, as a novel type of STE, exhibits an anomalous and complex structure due to deep convective injection into stratospheric intrusions and advection of remote marine air. The distinct mixture of stratospheric air and anthropogenic pollution alters the TCS, with horizontal and vertical scales estimated to be 200 and 1 km, respectively. Moreover, air of maritime origin, which is convectively transported and strongly dehydrated during long-range transport, is also identified. Such a complex TCS can produce unique chemical environments that modulate cloud physics and atmospheric radiation. An example is given in Figure 2. From a climatological perspective, events of these anomalous airmasses are nonnegligible in terms of their frequency and chemical impact, as revealed by multiyear observations. These new insights advance our understanding of the mixing of natural and anthropogenic species that shape the TCS in East Asia and have implications for climate change. (Chen et al., 2025)

Deep learning-based lightning nowcasting with embedded attention mechanisms. This study leverages the data-driven capabilities of deep learning to construct a multi-layer UNet neural network architecture with an embedded attention mechanism, resulting in the AME-UNet model for lightning nowcasting in North China. The structure of AME-UNet is shown in Figure 3. The model integrates lightning location data from the State Grid of China with high spatiotemporal resolution data from the FY-4A geostationary meteorological satellite. Brightness temperature channel differences, which effectively represent cloud-top development heights and freezing levels with clear physical significance, are introduced as predictors for pixel-wise lightning nowcasting for 0-1h and 1-2h timeframes. Results indicate that the AME-UNet model holds promising potential for lightning nowcasting, achieving a maximum hit rate of 0.46 and a false alarm rate of 0.29 for the 0-1 hour forecast, and a hit rate of 0.41 with a false alarm rate of 0.44 for the 1-2 hour forecast. This study offers innovative approaches to deep learning-based lightning

nowcasting, expanding the toolkit available for severe weather nowcasting (Wang et al., 2025a).

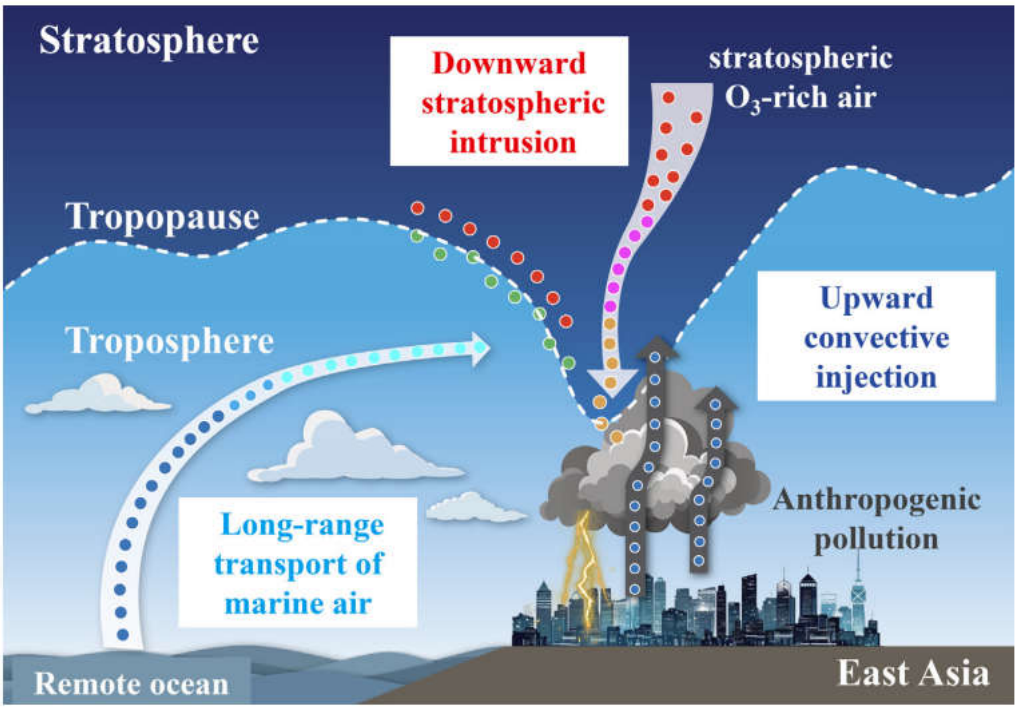

Figure 2. Conceptual scheme demonstrating the impact of two-way STE of stratospheric air and anthropogenic pollution and long-range transport of marine air on shaping the chemical structure of the tropopause region in East Asia.

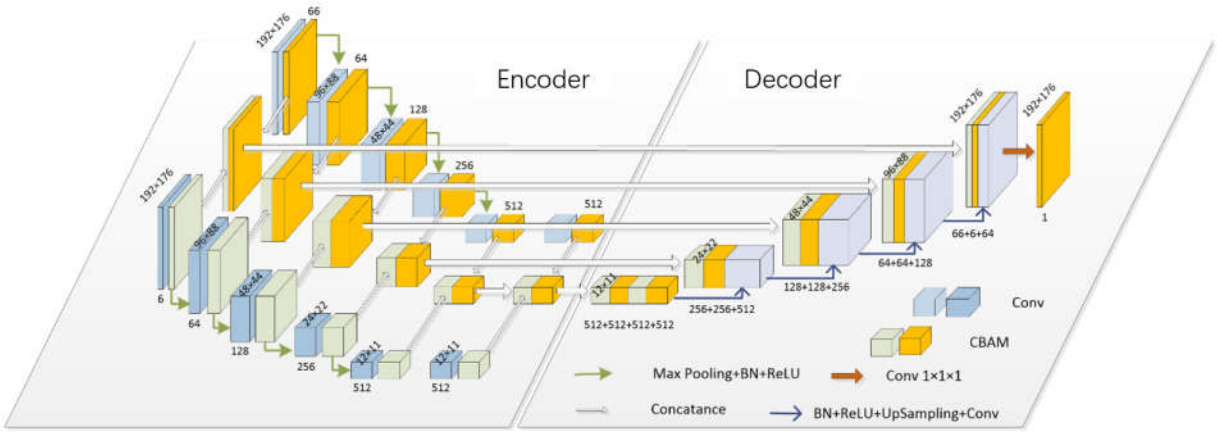

Figure 3. AME-UNet model structure. The left part of the model is the encoder, consisting of convolutional modules, max pooling modules, and attention mechanism modules. The right part corresponds to the encoder and serves as the decoder, composed of deconvolution modules and upsampling modules.

Infrared Brightness Temperature-Based Indicators for Identifying Thunderstorm Clouds: Insights from FY-4A Satellite Observations. Accurate monitoring and timely identification of early indicators of thunderstorms are of paramount importance in preventing and mitigating the potential disasters associated with such meteorological events. This study utilizes the TOBAC (Tracking and Object-Based Analysis of Clouds) automated tracking algorithm, integrated with FY-4A geostationary satellite infrared data, to investigate the spatial-temporal characteristics and evolutionary patterns of cloud-top brightness temperature (BT), areal extent, and phase transitions of thunderstorm and non-thunderstorm clouds across the North China region (Figure 4).

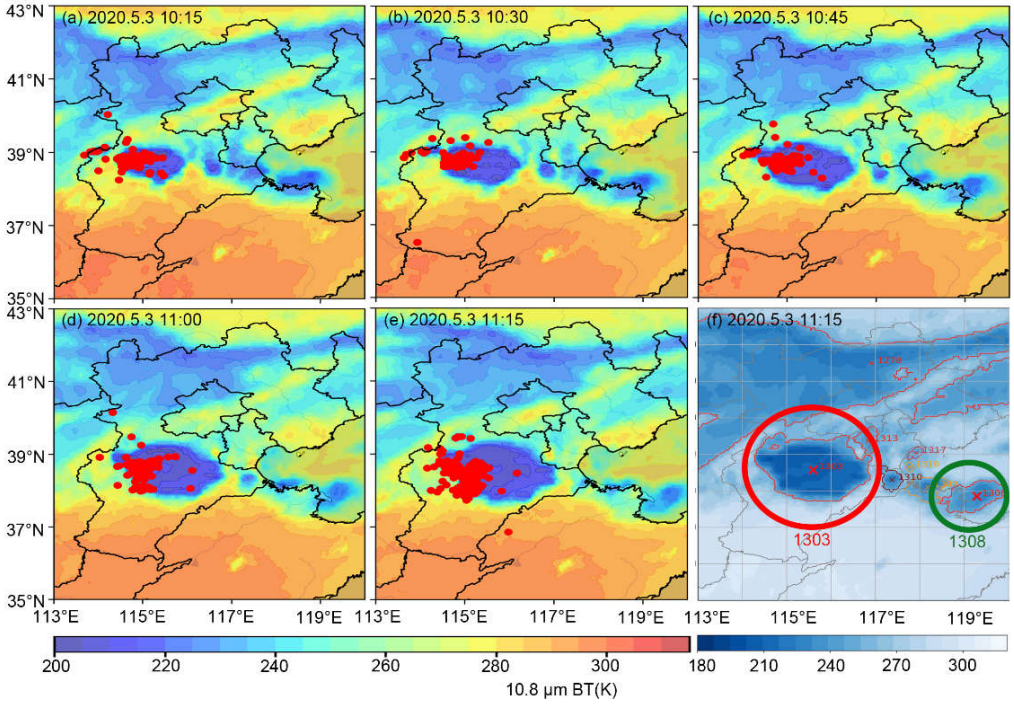

Figure 4. Thunderstorm evolution on May 3, 2020. (a-e) displays the BT map for the period from 10:15 to 11:15 on May 3, 2020, with color fill representing the 10.8 μm BT, and red scatter points indicating lightning locations. (f) illustrates the successful identification and tracking of thunderstorm (red circles) and non-thunderstorm (green circles) clouds by TOBAC.

The analysis reveals that thunderstorm clouds demonstrate significantly enhanced convective intensity compared to non-thunderstorm clouds, with the following distinctive features: (1) a substantially faster drop rate in 10.8 μm BT, reaching values nearly 2.3 times greater; (2) positive BT differences between 10.8 and 8.5 μm channels, exceeding 0 K; and (3) a dramatically increased areal expansion rate, approximately 4.5-fold higher than that observed in non-thunderstorm clouds. These findings provide

significant scientific insights and practical implications for advancing thunderstorm identification techniques and optimizing early warning systems, which are critical to improving disaster prevention and mitigation capacity across the North China region. An example of thunderstorm tracking evolution is given in Figure 4. (Wang et al., 2025b)

Jagiellonian University, Poland

Contributors: J. Kubisz, A. Michalec, Z. Nieckarz, M. Ostrowski, ELF@oa.uj.edu.pl

Studies of Extremely Low Frequency EM Waves. At the Astronomical Observatory of the Jagiellonian University in Kraków (Poland), a small geophysical group (https://www.oa.uj.edu.pl/elf) conducts studies of Extremely Low Frequency (ELF; defined here as the range 0.03–1000 Hz) electromagnetic waves (EW) using magnetic sensors installed at the Hylaty Station, located in an electromagnetically clean environment in southeastern Poland. The research is carried out in close collaboration with Dr. J. Mlynarczyk from the AGH University of Kraków. Together with our international partners, the group also operates the WERA array of magnetic sensors in Poland, the USA, and Argentina (https://www.oa.uj.edu.pl/WERA/).

Our main research topics focus on ELF EW propagation, ionospheric studies, and the influence of space weather on the studied processes. We are also part of the VIRGO gravitational wave (GW) observatory, where we investigate potential noise in GW measurements caused by coherent global magnetic fluctuations in the ELF range.

A significant part of the activity is devoted to operation and maintenance of magnetic sensors in ELF, which were developed by our group. Currently, a project is underway to upgrade the existing magnetic sensors at WERA stations. Both new antennas and new digital electronic receivers are being developed, aiming to upgrade the ELA11 digital magnetic sensor currently operated in Poland, which features 18-bit resolution and a 3 kHz sampling frequency.

Our recent studies include a directional analysis of ELF propagation of lightning impulses from thunderstorms. In the paper by Ostrowski et al. (2024a), we applied an approach — published in the beginning of 2024 — for deriving the azimuths of traveling ELF waves to reveal ionospheric variations, which manifested as day-to-day modifications of the daily azimuth distribution. A subsequent

paper (Ostrowski et al. 2024b) extended this approach by deriving individual propagation paths for WWLLN-detected discharges, allowing us to visualize ionospheric effects generated by a solar flare.

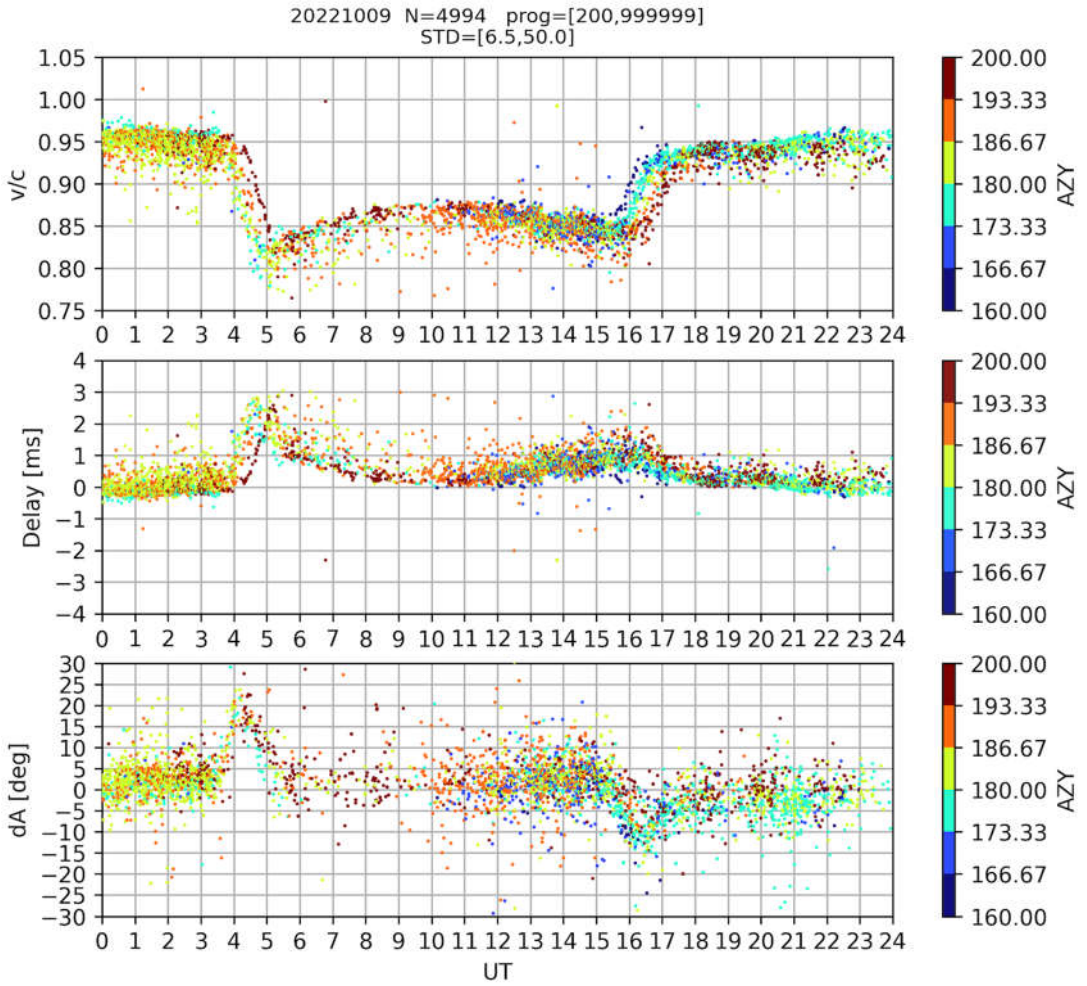

Figure 1. The 4994 ELF impulses identified for WWLLN-registered discharges in Africa.

These studies were continued primarily through the analysis of discharges detected globally by WWLLN in the VLF range, the discharges which generated EM impulses recorded by us in ELF. The first such study, by Nieckarz et al. (2025), compared ELF propagation conditions at different times of day and for various azimuths relative to the Hylaty Station, also revealing the influence of ionizing radiation from solar flares. The current research includes analysis of gamma-ray burst (GRB) effects on ELF EW propagation, as well as the study of positive and negative lightning discharges within the ones detected by WWLLN.

An illustration of such analysis is presented in the figure below, showing 4994 ELF impulses identified for WWLLN-registered

discharges in Africa with azimuths between 160° and 200° (see a color scale) and distances between 4,000 and 9,000 km. For each identified discharge, the figure shows — in the middle panel — it's delay with respect to the computed arrival time used for the ELF impulse identification. Then, on the top the derived propagation velocity in units of the speed of light, and in the bottom the deviation of the derived azimuths from the geographic azimuths of the original discharges are presented.

Massachusetts Institute of Technology

Analysis continues on the global ELF Q-burst dataset provided by Anirban Guha and Paul Nicholson, and enabled by the 6-station HeartMath network of ELF sensors. Dr. Qianqian Wang is considering the relationship between the background and the transient Schumann resonances on the diurnal and seasonal time scales, and chimney-by-chimney. The 8 Hz magnetic intensity in the Hew (Hns) field components at Hornsund station (in the Arctic) are used as reliable measures of the background intensity in Africa (Asia and America), respectively. The background signals are typically maximum near 4 pm local time in each lightning chimney (and later in Africa by 1-2 hours), consistent with the behavior of the total lightning activity (Blakeslee et al., 2014). The diurnal analysis is complicated by the consistent enhancement of Q-bursts in the vicinity of both the daytime and nighttime terminators, primarily on the dayside, and readily apparent by plotting Q-burst diurnal variations versus local time. The tentative finding is that the Q-burst maxima (with positive polarity events lagging negative polarity events) lag the SR background chimney maxima by 1-2 hours. The ELF background observations are also being checked with optical observations from the lightning Imager-detected flashes for the entire African continent generously supplied by Sven-Erik Enno from Eumetsat's MTG satellite.

The analysis of the background/transient interaction on the seasonal time scale has been shown to be more straightforward than the diurnal. The seasonal variability of monthly mean Q-burst counts shows an annual cycle similar with the global lightning activity (with NH summer maximum) and with a similar amplitude variation of a factor-of-two.

Analysis of B.F.J. Schonland's negative results in 1929 in searching for evidence of electron runaway is now complete in this collaborative work with Ashot Chilingarian, Hripsime Mkrtchyan and Gagik Hovsepyan, and has now been accepted in JGR. The dramatic contrast (14-fold) in prevalence of

thunderstorm ground enhancements (TGEs) between Aragats and Nor Amberd stations in Armenia makes it likely that the low station altitude in Schonland's Johanessburg (1780 m MSL) was attenuating the gamma radiation sufficiently in the intervening atmosphere to prevent event detection in the time period allotted for Schonland's search (9 thunderstorm days). Attenuation lengths for gamma rays (MeV range), are a few hundred meters—small in comparison with the altitude difference between Aragats (3200 m MSL, where TGEs are abundant) and Nor Amberd (2000 m MSL, where TGEs are scarce).

An opportunity has arisen with a power company in Italy (TERNA), coordinated by Prof Amedeo Andreotti at the University of Naples, to attempt the measurement of the air-earth current of the DC global circuit to a long (26 km) unenergized transmission line. The proposed effort follows earlier work in Hungary with Daniel Piri and Jozsef Bor on short distribution lines.

The manuscript by Yakun Liu et al. on the impact of the 2020 COVID pandemic in reducing the regional/global lightning activity, a presumed aerosol effect, has been accepted by the Journal of Geophysical Research.

Nanjing University of Information Science and Technology (NUIST), Nanjing, China

Numerical simulation study of the evolution of lightning channel decay and reactivation processes. Channel decay and reactivation are very common discharge phenomena, which have an important influence on the type, duration, and development of lightning discharges. However, how the electrical parameters in lightning channels change during reactivation processes and how reactivation affects the development of lightning leaders are still unclear. Researchers from Nanjing Innovation Institute for Atmospheric Sciences and Nanjing University of Information Science and Technology employed the two-dimensional self-sustained charge neutrality lightning model to simulate the discharge process of intracloud lightning flashes and conducted an extensive analysis of channel decay and reactivation processes. Our results suggest a close correlation between the length of reactivated channels and the distribution of channel electrical parameters, and the reactivation process has a significant influence on lightning channel development. Specifically, it is found that greater charge accumulation at the reactivation starting point and higher residual conductivity of the decayed channels can lead to longer

reactivated channels. And, the reactivation initiated from the positive leader end may both promote the resumption of the extension of the positive leader branch that has stopped extending and accelerate the propagation of an advancing positive leader. Moreover, reactivation may also activate the decayed negative leader channel, facilitating the lateral generation of new branches, which is crucial for the formation of hybrid lightning, needle-like structures, etc. The simulation results validate previous speculations from observation studies regarding the potential influence of the reactivation process on lightning channel development and lay the foundation for the subsequent use of this model to explore the differences between the reactivation process initiated from the positive and negative leader end. (Zheng et al, 2025, Journal of Geophysical Research: Atmospheres).

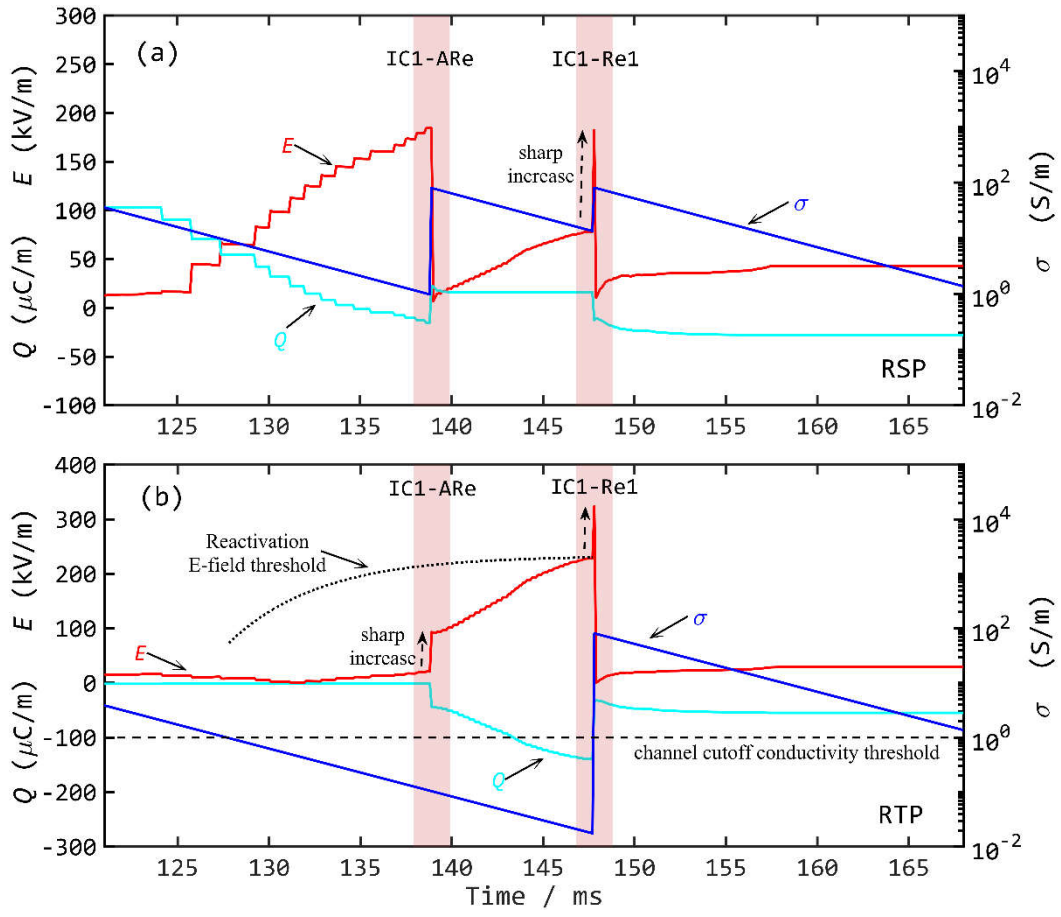

Figure 1. Temporal profiles of conductivity (σ), channel E-field (E), and line charge density (Q) at the starting point RSP (a) and the termination point RTP (b) of the attempted reactivation IC1-ARe. The red, blue, and cyan curves represent E, σ, and Q, the dotted line and the dashed line represent the reactivation E-field threshold and the channel cutoff conductivity threshold, respectively.

Effects of aerosols on diurnal variation of lightning activity in the Sichuan Basin, China. Aerosol can affect the lightning activity through radiative and microphysical effects. This study attempts to reveal the distinct impact pathways of these two effects on lightning activity. Using data of cloud-to-ground (CG) lightning, aerosol optical depth (AOD), thermodynamic, and cloud-related variables during the summer (June, July, and August) of 210-2018 in the Sichuan Basin, we investigate the changes in the diurnal variation of lightning activity characteristics between the polluted (2010-2013) and clean (2015-2018) years. Polluted years exhibit more thunderstorms during the late afternoon and early evening hours than clean years, but show no significant differences in other time periods. During all time periods, thunderstorms in polluted years are more intense, with a higher CG lightning density. Aerosols exhibit more intense radiative effect during afternoon and early evening hours in polluted years, which reduces the surface temperature, thereby enhancing atmospheric stability and inhibiting the formation of convection. The cloud liquid water and cloud ice water content in polluted years are higher, suggesting stronger aerosol microphysical effects. These results indicate that the radiative effects of aerosols primarily influence lightning activity by altering the frequency of thunderstorms, whereas the microphysical effects of aerosols predominantly affect lightning activity by modulating the intensity of thunderstorms. (Wang et al, 2025, Atmospheric Research).

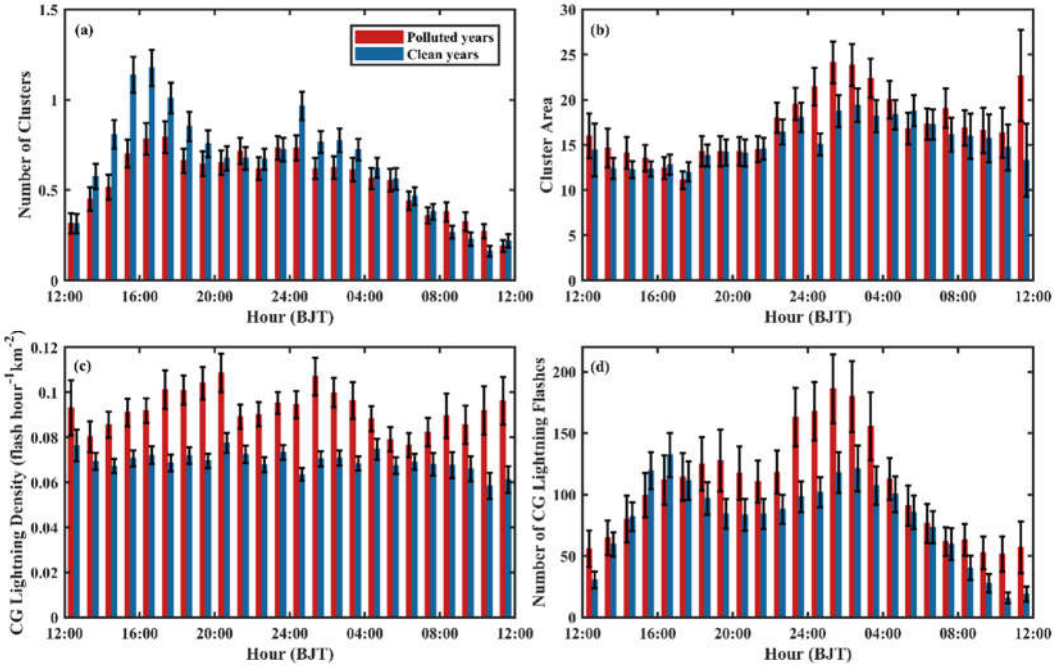

Figure 2. Diurnal variations of (a) mean number of clusters, (b) mean cluster area, (c) mean CG lightning density, and (d) mean number of CG lightning flashes in polluted and clean years for normal samples. The I-type vertical bars indicate the standard error in each hour.

NOAA/OAR National Severe Storms Laboratory

Hurricane Ian Observations. The initial publication detailing the targeted observations our group collected during the landfall of Hurricane Ian, a Category 5 hurricane just prior to its landfall in Florida during September 2022, has been accepted for publication (Ringhausen et al., 2025). Measurements included a Lightning Mapping Array, X-band radar, radiosondes profiles, and surface observations. This storm contained intense eyewall convection, resulting in impressive mixed-phase precipitation and lightning generation prior to landfall.

PAPEL. The Phased Array Polarimetric Electrification Lightning (PAPEL) project, funded through NSF's EAGER program, has made advances in our ability to observe lightning processes within severe storms. A central focus of the project is leveraging the unique capabilities of the fully digital Horus S-band polarimetric phased array radar to observe lightning-induced plasma echoes and their associated polarimetric signatures at unprecedented spatiotemporal resolution.

A key scientific milestone was the publication of Vitor Goede et al. (2025), which documents the first-ever rapid-scan observations of total lightning flashes using a polarimetric phased array radar. The study analyzed more than 580 lightning echoes sampled during severe storms in central Oklahoma. These echoes were strongly correlated in space and time with lightning mapping array (LMA) sources and were characterized by distinct transient changes in radar variables: increased horizontal reflectivity (ZH), broadened and variable differential reflectivity (ZDR), large phase fluctuations in ΦDP, and reduced correlation coefficient (ρHV). These signatures support the interpretation that the radar beam was intercepting hot, overdense plasma associated with propagating lightning channels.

Figure 1. The Horus radar deployed in the parking lot of OU's Lloyd Noble Center on 28 April 2024 (around 2:00 UTC), capturing data amid intense lightning activity and several tornadic storms in the region.

As part of PAPEL, the team implemented and deployed a novel 2D beam spoiling mode with the Horus radar, enabling rapid full-volume scans every 3.5 seconds. This scanning strategy significantly improved temporal resolution compared to conventional radars and allowed for the observation of flash-scale phenomena, such as lightning initiation and propagation. Additional work under PAPEL has included the refinement of lightning detection algorithms, development of a simulation framework for electric field estimation from negative KDP signatures, and validation of radar observations using LMA data.

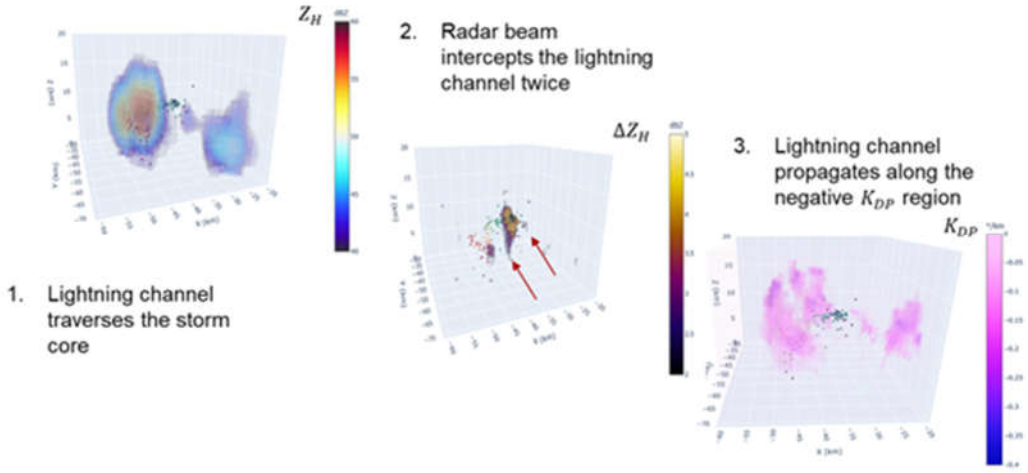

Figure 2. Three-dimensional renderings from Horus radar volume scans, illustrating (left) horizontal reflectivity factor (ZH), (center) the change in reflectivity (ΔZH), and (right) specific differential phase (KDP). Overlaid black dots mark LMA-detected lightning sources, while red arrows in the center panel highlight regions of notable reflectivity changes associated with lightning activity.

These integrated efforts—combining radar hardware innovation, algorithm development, and coordinated field observations—are helping to build a deeper understanding of storm electrification processes and lightning physics. The project also lays important groundwork for the future operational use of polarimetric phased array radar data to detect lightning and improve convective storm diagnosis.

Graduate Projects. We had two students complete their projects for their graduate degrees this spring. A brief summary of each follows below.

Kevin Thiel's Dissertation. Machine learning methods for assessing the probability of lightning activity and thunderstorm intensity are becoming commonplace in both operational and severe storms research fields. Integrated, multi-tiered models which leverage

information from both satellite imagery and radar have been less explored. A two-tired machine learning problem was posed to identify convection based on the presence of lightning activity (tier 1) and then classify convection as intense based on local lightning flash rates (tier 2) using observations from the GOES-R Geostationary Lightning Mapper. Two random forests were trained in tandem on only four radar and satellite variables, and from seven cases of warm-season convection in the Continental United States, to coincide with results from previous studies. Isothermal reflectivity at the -10°C isotherm demonstrated the greatest importance for both models. When identifying convection 10.3 μm infrared brightness temperatures less than 220 K and -10°C isothermal reflectivity values greater than 23 dBZ were frequently associated with lightning activity, even at low probabilistic thresholds from the tier 1 random forest model. When identifying convection capable of producing robust local flash rates, the tier 2 random forest model demonstrated that -10°C isothermal reflectivity greater than 30 dBZ were frequently associated with more intense convection. Lastly, a case study of a thunderstorm from 14 May 2022 demonstrated the capability of both tiers of the model to provide diagnostic information for thunderstorm activity and intensity.

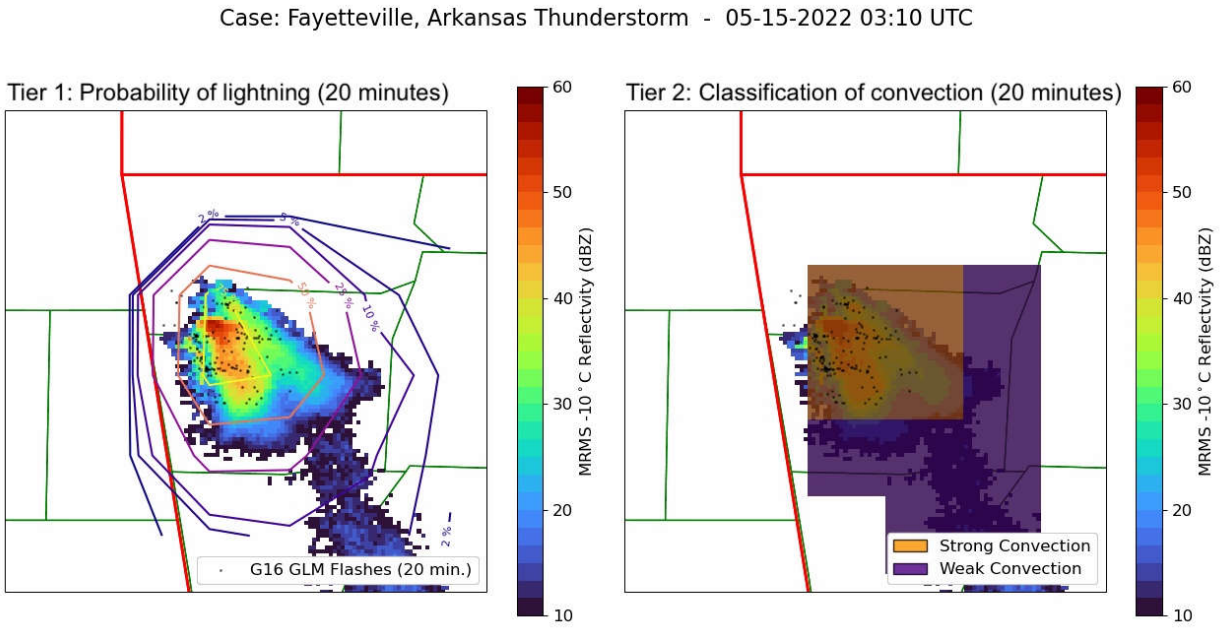

Figure 3. Output from the Tier 1 and Tier 2 random forest models for a thunderstorm near Fayetteville, Arkansas on 15 May 2022 at 0310 UTC, showing the probability of lightning (left) and classification of each pixel as strong (orange) and weak (purple).

Christopher Schneider's Thesis. Mobile balloon launches at The National Oceanic and Atmospheric Administration (NOAA) National Severe Storms Laboratory (NSSL) are vital for upper air data sources and in situ observations. To constrain the distance flown by the package, as well as limit potential damage sustained to sensors, a cutdown mechanism releases the instrument package from the balloon. The package also features a letdown system to increase the distance between the sensor package and balloon once in flight to reduce the influence of the balloon on the measurements. This research project presents a prototype hook and latch mechanism for the cutdown application ensuring ease of use and improved operational capabilities. A comprehensive analysis of all designed geometries was carried out using Ansys engineering software for finite element analysis (FEA), SOLIDWORKS modeling, drop testing of parts, video analysis, and theoretical force calculations. The methodology presented in this study produces a successful mechanism optimized for deployment in various severe weather field applications.

School of Earth and Space Sciences, University of Science and Technology of China (USTC), Hefei, China

Massive outbreak of red sprites in South Asia observed from the Tibetan Plateau. On May 19, 2022, an outbreak of 105 red sprites occurring over South Asia was fortuitously recorded by two amateurs from a site in the southern Tibetan Plateau (TP), marking the highest number captured over a single thunderstorm in South Asia. Nearly half of these events involved dancing sprites, with additional 16 uncommon secondary jets and at least 4 extremely rare green emissions called "ghosts" followed the associated sprites. Due to the absence of precise timing needed to identify parent lightning, a method based on satellite motion trajectories and star fields is proposed to infer video frame timestamps with an error of less than 1 second. After verifying 95 sprites from two videos, the method identified the parent lightning for 66 sprites (~70%). The sprite-producing strokes, mainly of positive polarity with exceeding +50 kA, occurred in the stratiform region of a mesoscale convective complex (MCC) that spanned from the Ganges Plain to the southern TP, with a cloud area over 200,000 km^2 and a minimum cloud-top black body temperature near 180 K. The observation confirms that thunderstorms in South Asia, akin to

mesoscale convective systems (MCSs) in the Great Plains of the United States or coastal thunderstorms in Europe, can produce sprites in a great amount, including complex species (H. Huang et al., 2025, Adv. Atmos. Sci.).

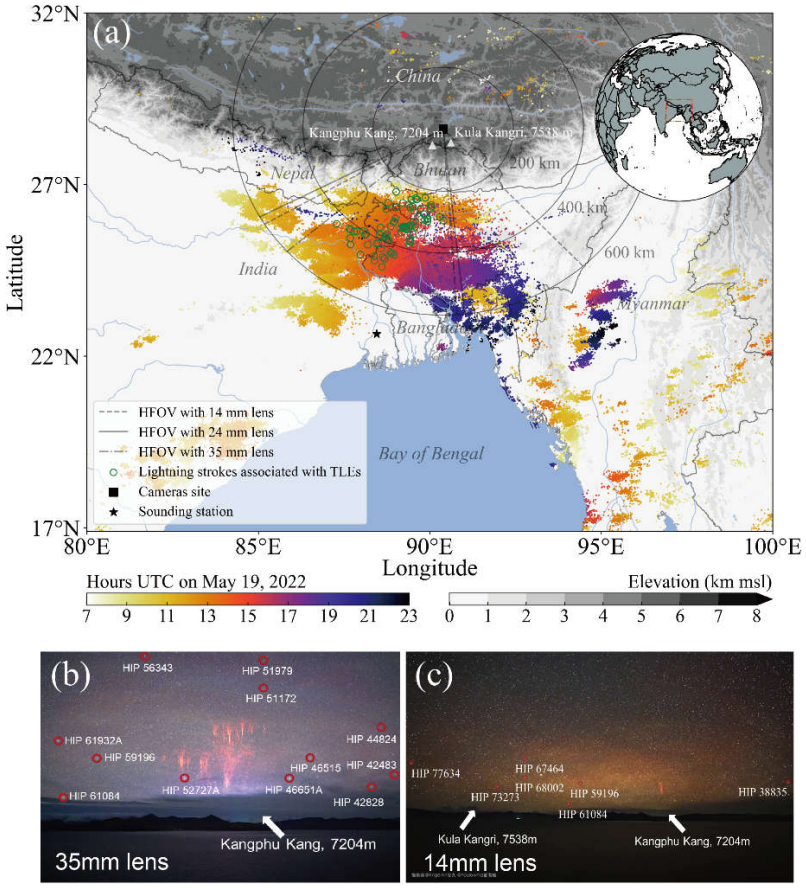

Figure 1. (a) Overview of the observation, the colored dots denote the locations of the GLD360 lightning strokes from 0700-2300 UTC. Panels (b) and (c) show the field of view with the 35-mm lens and the 14-mm lens, respectively, and their background star fields which marked their numbers in the Hipparcos Catalogues.

Ground-based observations of ghost green emissions and analyses of their excitation background. Ghosts are a newly discovered category of transient luminescence events (TLEs) occurring in the middle and upper atmospheres above energetic thunderstorms. Due to the high requirements of optical shooting, the observation data that can be investigated are very scarce and are all obtained from the ground-based observations at a single station. Based on the ground-based observation of seven ghost events with original optical data, in this paper we present a methodology to estimate the altitude of ghosts from single-station observation in conjunction with star-field background, and determine the altitude range of five ghosts (two of which are at the same place and time) to be 90 to 100 km. So far, ghost events are known to be accompanied with two different types of TLEs,

namely "red sprite" or "gigantic jet". The accompanying relationship between ghost events and these two TLEs shows that the occurrence of ghost events may be closely related to the altitude and the strong electric field and energy release during the thunderstorm. This paper further examined the atmospheric background conditions (i.e., neutral particle density, ion concentration and electron density, etc.) upon the observations of the aforementioned seven ghost events. The density profile of neutral particles (O, N2, O2), ion (O2+ and NO+) and electron density were obtained by means of the MSIS-E-90 model and the IRI model. It was found that the mutation of N2, O2 and electron density played a key role in the occurrence of ghosts. These mutations of density may provide necessary medium conditions for the occurrence of ghosts. In this paper, by calculating the diffusivity of ghosts, it is found that the diffusivity of ghost is much lower than that of streamer discharge, which confirms that ghost emission is a form of glow discharge. Finally, the characteristics of the parent thunderstorms of ghosts are analyzed, and it is found that ghosts occur in the phase of weakening convective activity, which implies that the formation of ghost might require the existence of lightning flashes with relatively high energy release. In the weakening stage of thunderstorm activity, although the convective activity decreases, the electric field of the thunderstorm cloud top may still be strong, thus providing the necessary energy conditions for the occurrence of ghost events. (X. Huang et al., 2025, Reviews of Geophysics and Planetary Physics, in Chinese).

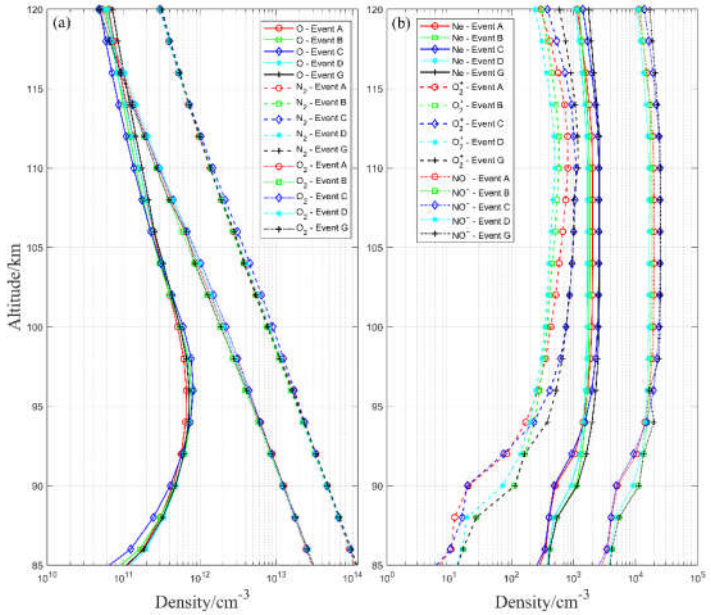

Figure 2. Gradient of background density. (a) neutral density profiles, including atmospheric constituents (O, N_2, O_2) from the MSIS-E-90 model. (b) charged particle density distribution (Ne，O_2^+，NO^+) from the IRI model.

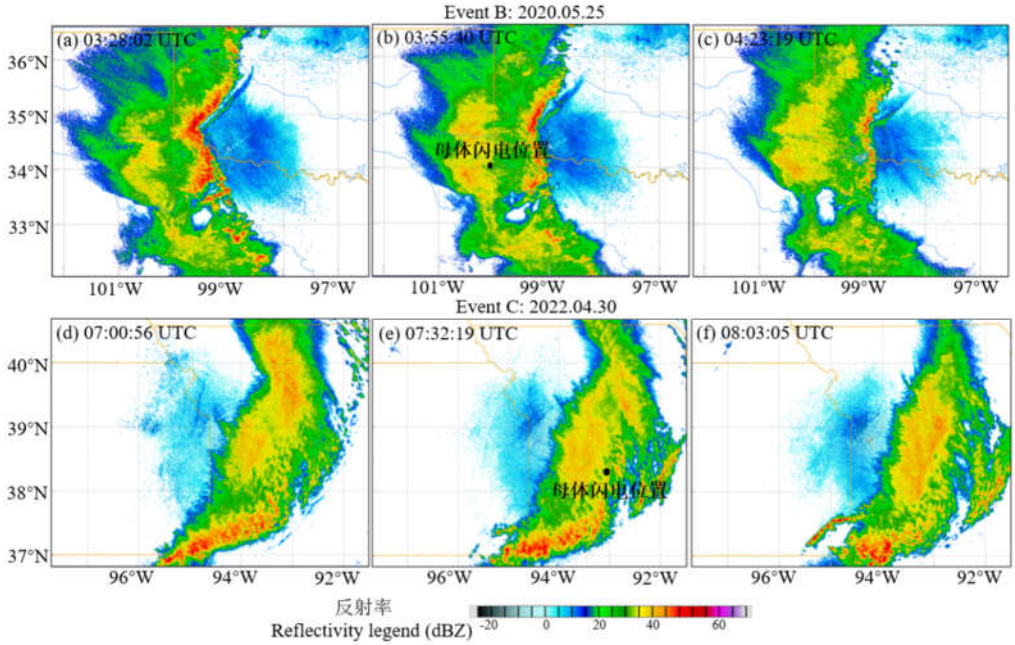

Figure 3. NEXRAD Level-II radar scan (elevation angle is 0.48°) of base reflectivity for the parent thunderstorm of ghost. The black dot marks the location of the parent stroke of the red sprite associated with ghost. Event B: (b) is when ghost occurred; (a) and (c) are 30 minutes before and after ghost. Event C: (e) is when ghost occurred; (d) and (f) are 30 minutes before and after ghost.

Ionospheric elves powered by corona discharges in overshooting thunderclouds. Corona discharges in thundercloud tops are observed by the Atmosphere-Space Interactions Monitor (ASIM) as blue flashes at the 337 nm spectral line of N_2 and by ground receivers as so-called Narrow Bipolar Events (NBEs) in the radio signals. Theoretical studies have proposed that electromagnetic radiation from these discharges might be powerful enough to excite "elves"—rapidly expanding luminous rings in the lower ionosphere. However, experimental evidence for this hypothesis has been absent. In this study we provide the first concurrent observational evidence, using the ASIM aboard the International Space Station and ground-based sferic arrays in China, confirming that intense negative NBEs (impulsive intracloud discharges) near cloud tops can indeed generate elves in the lower ionosphere (70–100 km altitude). Observations indicate that elves are triggered when the absolute peak current of these negative NBEs exceeds approximately 140 kA. These rare blue discharges, typically located near or at the edge of overshooting cloud tops within strong convective systems (as observed in Tropical Storm Maysak and a Bay of Bengal storm), highlight a connection between deep convective surges and upper atmospheric electrical phenomena. Additionally, the study

demonstrates that the brightness of associated blue optical emissions correlates with the discharge peak current, providing an alternative method for estimating the currents of these powerful corona discharges impacting the middle atmosphere. This discovery expands the known sources of ionospheric perturbations beyond cloud-to-ground lightning, emphasizing a previously underappreciated mechanism of atmospheric coupling. It also has potential implications for understanding greenhouse gas perturbations at the tropical tropopause. (F. Liu et al., 2025, Geophys. Res. Lett.)

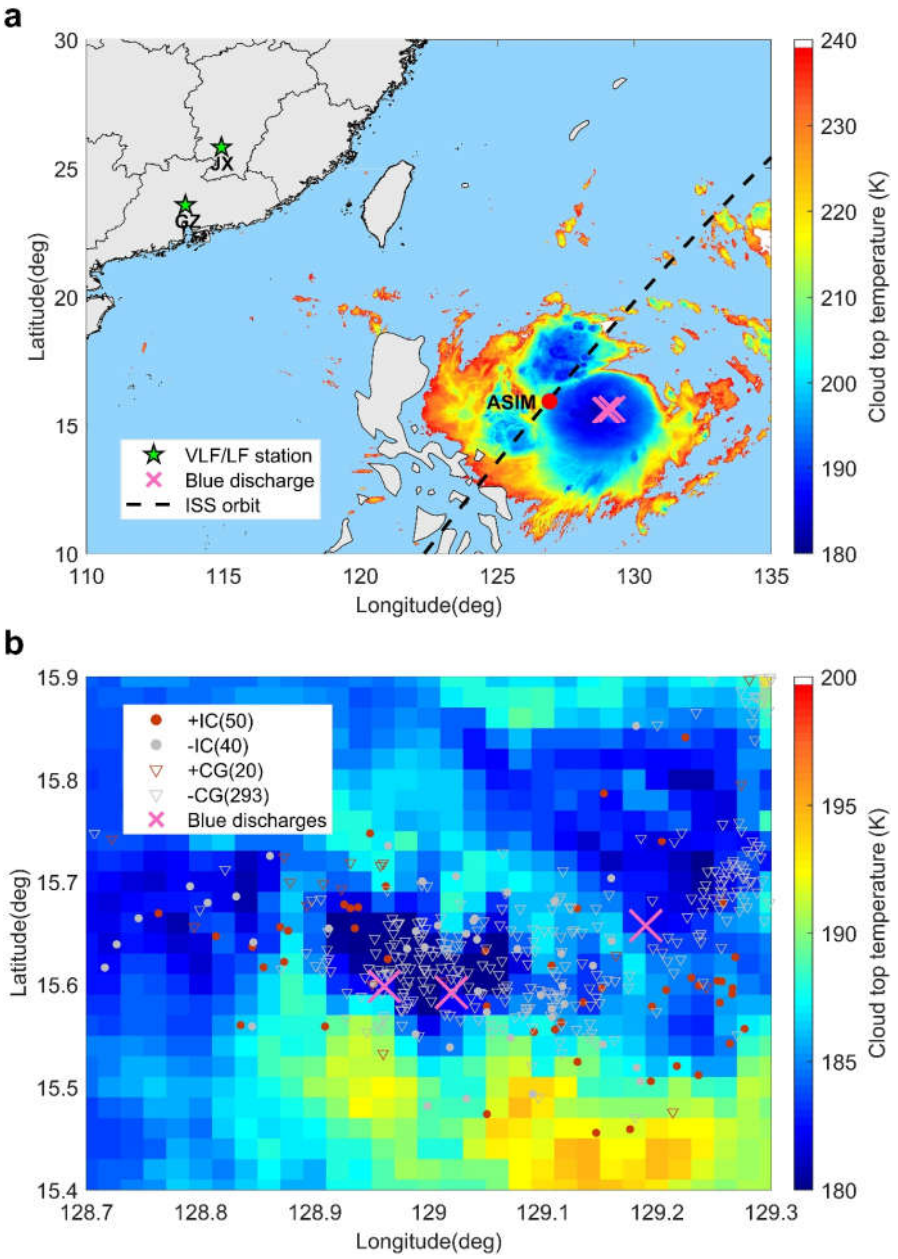

Figure 4. Tropical storm Maysak on 28 August 2020 with three blue discharges. The cloud top temperatures at 17:10 UTC provided by Himawari-8 satellite data and the location of the fast blue

discharges (pink crosses) from ASIM camera data projected to 19 km altitude corresponding to a cloud top temperature of 180 K. (a) The dashed line is the ISS orbit and the red marker its position at 17:13 UTC when the three blue discharges were observed. The fields of view of ASIM photometer and camera corresponding to the overpass time at 17:13:11 UTC are shown in circle and square, respectively. The green stars mark the location of the VLF/LF stations measuring the associated NBEs. (b) Zoom to the active region. CGs and IC lightning activity during 17:00–17:30 UTC obtained by the GLD360 network are superimposed.

University of Florida

Z. Ding, V. A. Rakov, Y. Zhu, S. Chen, and I. Kereszy authored a paper titled "Positive and negative lightning leaders imaged in UV and visible ranges". Based on their recent observations at the Lightning Observatory in Gainesville (LOG), Florida, the authors presented, for the first time, ultraviolet (UV, 290-370 nm) images of positive and negative lightning leaders in CG flashes along with the simultaneously recorded visible (400-800 nm) images. The distances ranged from 5 to 11 km. The key findings include the discovery of a pulsating streamer zone at the *positive* leader tip in UV, while no streamer zone was detectable in the visible. The streamer zone at the *negative* leader tip was undetectable in either UV or visible ranges. The observed polarity asymmetry is likely to be related to very different (orders of magnitude) streamer production rates at positive and negative leader tips. As examples, UV records of 2 positive (red boxes) and 2 negative (blue boxes) leaders, which illustrate the difference in detectability of positive and negative streamer zones, are shown below. The 2 negative events are weaker in terms of the NLDN-reported return-stroke peak current, but they are recorded at closer distances, so that the effect of stronger source is somewhat compensated by stronger attenuation in propagation to the receiver.

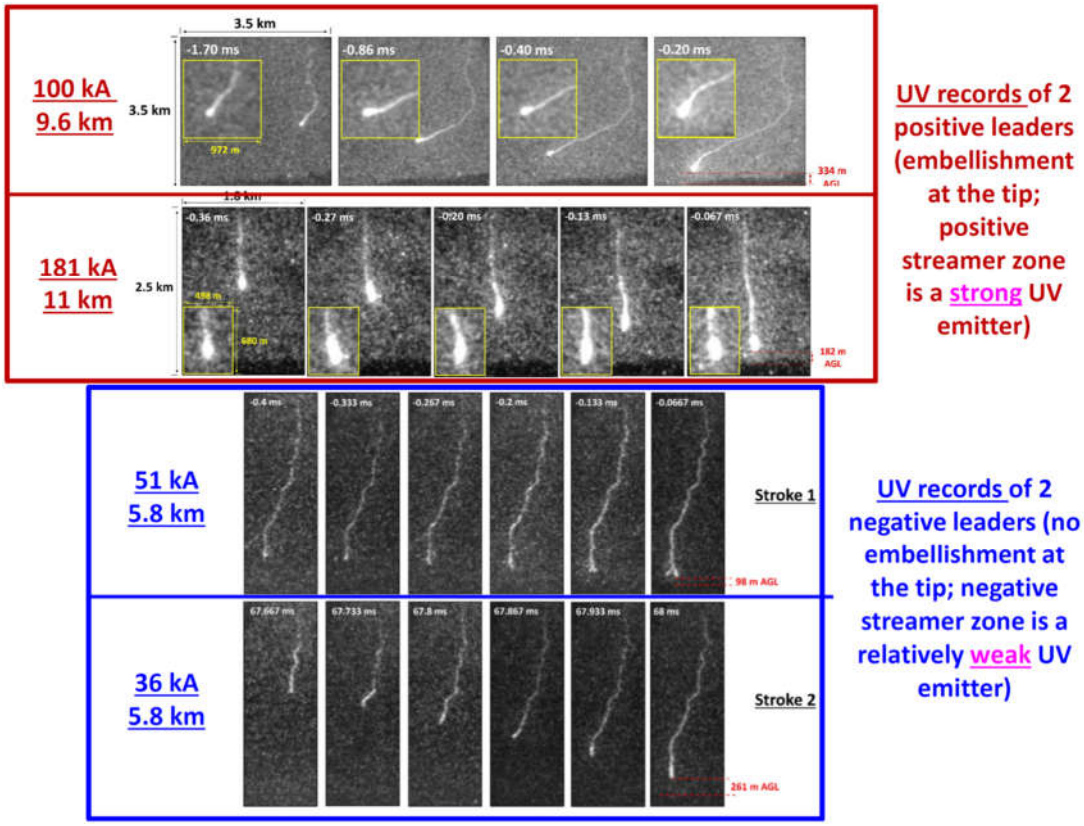

Figure 1. The quasi-periodic fluctuations (pulsations) of the size of the positive-leader streamer zone observed in UV had a period of roughly 100 μs, which is comparable to the range of 40-120 μs reported by Berger and Vogelsanger (1966) for the visible luminosity fluctuations of the channels of upward positive leaders initiated from their towers in Switzerland. Ding et al. offered a hypothetical mechanism of the positive streamer zone pulsation. This paper is published in the Geophysical Research Letters.

This list of references is not exhaustive. It includes only papers published during the last six months provided by the authors or found from an on-line research in journal websites. Some references of papers very soon published have been provided by their authors and included in the list. The papers in review process, the papers from Proceedings of Conference are not included.

Abbott T H, N Jeevanjee, K-Y Cheng, L Zhou, L Harris. 2025. The land-ocean contrast in deep convective intensity in a global storm-resolving model. J Adv Model Earth Syst, 17, e2024MS004467. doi:10.1029/2024MS004467.

Biswasharma R, M A Domkawale, R Ghosh, A Gangane, N Umakanth, et al. 2025. Assessment of the Indian Lightning Location Network (ILLN) using ground-based and satellite observations. Atmos Res, 320, 108069. doi:10.1016/j.atmosres.2025.108069.

Bozoki T, J Mlynarczyk, P Prácser, et al. 2025. Modelling the global electromagnetic resonance field produced by lightning discharges with a continuing current. ESS Open Archive, doi:10.22541/essoar.174326612.28669941/v1.

Cai L, M Chen, T Han, M Zhou, J Cao, et al. 2025. The relationship between cloud-to-ground lightning spatial distribution and topography in Guangzhou. J Atmos Sol-Terr Phy, 273, 106554. doi:10.1016/j.jastp.2025.106554.

Chen Z, J Su, J Liu, X Qie, V Thouret, et al. 2025. Convective injection into stratospheric intrusions alters the tropopause chemical structure. Science Bulletin, 70, 1328-1337. doi:10.1016/j.scib.2024.12.053.

Choudhury B A, M I R Tinmaker. 2025. Thermodynamic control of lightning activity in premonsoon and monsoon season over the Indian region. J Atmos Sol-Terr Phy, 268, 106410. doi:10.1016/j.jastp.2024.106410.

Ding J, W Zhang, D Zheng, Y Zhang, W Yao, et al. 2025. Thunderstorm structure and lightning properties in South China and over the South China Sea: A comparative study. J Meteorol Res, 39, 415–430. doi:10.1007/s13351-025-4091-8.

Ding Z, V A Rakov, Y Zhu, S Chen, I Kereszy. 2025. Positive and negative lightning leaders imaged in UV and visible ranges. Geophys Res Lett, 52, e2024GL113689. doi:10.1029/2024GL113689.

Dodge S, M Nicora, S Barmada, M Brignone, R Procopio, et al. 2025. A deep learning based lightning location system. Electr Pow Syst Res, 242, 111437. doi:10.1016/j.epsr.2025.111437.

Düzgün C, H Fuelberg, R Adams-Selin, N Heath. 2025. Evaluating the effectiveness of lightning data assimilation in parameterized deep convection. Mon Wea Rev, doi:10.1175/MWR-D-24-0221.1.

Dwyer J R. 2025. Energetic particles produced by thunderstorm electric fields. J Geophys

Res Atmos, 130, e2024JD042193. doi.org/10.1029/2024JD042193.

Fischer G, M Imai, U Taubenschuss, D Pisa, W S Kurth. 2025. The radio wave polarization of saturn lightning observed by Cassini. J Geophys Res Space Phys, 130, e2024JA033560. doi:10.1029/2024JA033560.

Gangane A, P Priyadarshini, S D Pawar, H A Syed, R Biswasharma, et al. 2025. Falling trend of winter lightning over western India and its possible relation with western disturbances. Earth Space Sci, e2024EA003726. doi:10.1029/2024EA003726.

Goede V, D Schvartzman, D Bodine, V C Chmielewski, T-Y Yu, et al. 2025. Rapid sampling and polarimetric statistics of lightning with a phased array radar. Geophys Res Lett, 52, e2024GL112193. doi:10.1029/2024GL112193.

Goenka R, A Taori, G S Rao, P Chauhan. 2025. Leveraging INSAT-3D Indian geostationary satellite for advanced lightning detection and analysis. Geophys Res Lett, 52, e2024GL112764. doi:10.1029/2024GL112764.

He Z, J Yu, X Ding, et al. 2025. Latitudinal distribution and propagation of lightning-generated whistler: A statistical study by Van Allen Probes observation and ray-tracing simulation. Sci. China Earth Sci., 68, 1291–1297. doi:10.1007/s11430-024-1535-5.

Honda R H, E A Kherani, C A O B Figueiredo, E Astafyeva, C M Wrasse, et al. 2025. Resonant infrasonic disturbances in total-electron-content during a severe thunderstorm on 23 October 2021. J Geophys Res Space Phys, 130, e2024JA033679. doi:10.1029/2024JA033679.

Huang H, G Lu, A An, et al. 2025. Massive outbreak of red sprites in South Asia observed from the Tibetan Plateau. Adv Atmos Sci, 42, 1247–1260. doi:10.1007/s00376-024-4143-5.

Huang S, D Zheng, Y Zhang, Y Zhang, C Wu, W Yao, W Zhang. 2025. Evolution of charge structure in a thunderstorm over South China. Atmos Res, 322. doi:10.1016/j.atmosres.2025.108142.

Iudin D I, N L Aleksandrov, A A Syssoev, A A Ponomarev. 2025. Numerical simulation of lightning channel reactivation in recoil leader process. Atmos Res, 323, 108187. doi:10.1016/j.atmosres.2025.108187.

Karnas G, G Maslowski, V A Rakov. 2025. Frequency spectra features of electric field waveforms produced by close and middle-range compact intracloud discharges and their discrimination from cloud-to-ground lightning. Electr Pow Syst Res, 243, 111498. doi:10.1016/j.epsr.2025.111498.

Kato M, Y Tachibana, S Kasuga, H Sato, E Shigeta, et al. 2025. Influence of the Kuroshio system and its large meander on the incidence and interannual variation in lightning strokes. J Clim, doi:10.1175/JCLI-D-24-0123.1.

Khansalari S, M Gharaylou. 2025. Lightning prediction in the Tehran region using the WRF model with multiple physical

parameterizations and an ensemble approach. Earth Space Sci, 12, e2024EA004097. doi:10.1029/2024EA004097.

Kolmašová I, O Santolík, A Kolínská, et al. 2025. Rapid evolution of energetic lightning strokes in Mediterranean winter storms. npj Clim Atmos Sci, 8, 71. doi:10.1038/s41612-025-00965-6.

Kondo M, Y Sato. 2025. Transition of dominant cloud microphysical processes for increasing lightning preceding downbursts in multi-cell convective clouds. Atmos Res, 324, 108203. doi:10.1016/j.atmosres.2025.108203.

Kühne T, B Antonescu, P Groenemeijer, T Púčik. 2025. Lightning fatalities in Europe (2001–20). Weather, Climate, and Society, 17. doi:10.1175/WCAS-D-24-0038.1.

Li F, J Li, S Gu, Y Wang, Z Li, et al. 2025. Nowcasting of cloud-to-ground lightning location and frequency based on a deep learning technique. Atmospheric and Oceanic Science Letters, 100607. doi:10.1016/j.aosl.2025.100607.

Li X, Z Li, X Li, X Zhang, Y Chang, et al. 2024. Positioning of lightning electromagnetic radiation sources with satellite constellations: Simulation and preliminary validation. Earth Space Sci, 12, e2024EA004084. doi:10.1029/2024EA004084.

Li Z, H Zhang, J Hu, Y Zhang, J Yao. 2025. Research on the correlation between meteorological radar echo characteristics and lightning warning technology. Atmospheric and Oceanic Science Letters, 100649. doi:10.1016/j.aosl.2025.100649.

Liao Z, Y Han, L Li, Y Wu, F Yu, et al. 2025. Statistical analysis of the spatio-temporal characteristics of multiple return strokes cloud-to-ground lightning parameters in Guangdong Province, China. Atmos Res, 323, 108170. doi:10.1016/j.atmosres.2025.108170.

Lima J M S, E P Vendrasco, T S Biscaro. 2025. Study of lightning occurrence in the southeastern Brazil and its relationship with polarimetric variables observed by meteorological radar. Atmos Res, 323, 108189. doi:10.1016/j.atmosres.2025.108189.

Liu F, T Neubert, O Chanrion, N Liu, B Zhu, et al. 2025. Ionospheric elves powered by corona discharges in overshooting thunderclouds. Geophys Res Lett, 52, e2024GL114090. doi:10.1029/2024GL114090.

Liu Y, E Williams, A Guha, G Satori, O P Neto, et al. 2025. Reduction in global lightning activity during the COVID pandemic. J Geophys Res Atmos, 130, e2024JD042319. doi:10.1029/2024JD042319.

Liu Y, J Wang, Y Song, S Liang, M Xia, et al. 2025. Lightning nowcasting based on high-density area and extrapolation utilizing long-range lightning location data. Atmos Res, 321, 108070. doi:10.1016/j.atmosres.2025.108070.

Logan T, J Hale, S Butler, B Lawrence, S Gardner. 2024. Occurrence of rare lightning events during Hurricane Nicholas (2021). Earth Space Sci, 11, e2024EA003733. doi:10.1029/2024EA003733.

Luque A, D Li, I Bjørge-Engeland, N G Lehtinen, M Marisaldi, et al. 2025. Cumulative effects of lightning electromagnetic pulses on the lower ionosphere. J Geophys Res Atmos, 130, e2024JD042121. doi:10.1029/2024JD042121.

Mach D M, M G Bateman. 2025. Reintroducing single group flashes to improve Geostationary Lightning Mapper detection efficiency. J Geophys Res Atmos, 130, e2025JD043313. doi:10.1029/2025JD043313.

Ma R, D Zheng, Y Zhang, W Yao, W Zhang, B Zhu. 2024. Thunderstorms with extreme lightning activity in China: Climatology, synoptic patterns, and convective parameters. Remote Sensing, 16(24), 4673. doi:10.3390/rs16244673.

Marisaldi M, N Østgaard, A Mezentsev, T Lang, J E Grove, et al. 2024. Highly dynamic gamma-ray emissions are common in tropical thunderclouds. Nature 634, 57–60. doi:10.1038/s41586-024-07936-6.

Mittermaier M P, J M Wilkinson. 2025. Quantifying observation representativeness errors using a spatial verification method: A lightning-based illustration. Weather Forecast, doi:10.1175/WAF-D-23-0049.1.

Nieckarz Z, M Gołkowski, J Kubisz, M Ostrowski, A Michalec, et al. 2025. Monitoring global ionospheric conditions with electromagnetic lightning impulses registered in extremely low frequency measurements. Radio Science, doi:10.1029/2024RS008140.

Nussbaumer C M, A Pozzer, M Hewson, L Ort, B Krumm, et al. 2025. Low tropospheric ozone over the Indo-Pacific warm pool related to non-electrified convection. Geophys Res Lett, 52, e2024GL112788. doi:10.1029/2024GL112788.

Østgaard N, A Mezentsev, M Marisaldi, J E Grove, M Quick, et al. 2024. Flickering gamma-ray flashes, the missing link between gamma glows and TGFs. Nature 634, 53–56. doi:10.1038/s41586-024-07893-0.

Ostrowski M, M Gołkowski, J Kubisz, A Michalec, J Mlynarczyk, et al. 2024a. Refraction of ELF electromagnetic waves by the ionospheric gradients at the day/night terminator measured at the Hylaty station. J Geophys Res Space Physics, doi:10.1029/2024JA033274.

Ostrowski M, M Gołkowski, J Kubisz, Z Nieckarz, A Michalec, et al. 2024b. Effects of a solar flare on global propagation of extremely low frequency waves. J Geophys Res Space Physics, doi:10.1029/2024JA033083.

Peterson M. 2025. The Americas' mightiest megaflashes: A look at where the most extraordinary lightning occurs. Bull Am Meteorol Soc, 104, doi:10.1175/BAMS-D-20-0178.A.

Pilipenko V A, S E Smirnov, A V Frank-Kamenetsky, et al. 2024. An electrical storm during a magnetic storm on April 5, 2010. Izv. Atmos. Ocean. Phys. 60, 1247–1258. doi:10.1134/S0001433825700483.

Qi Q, B Wu, F Lyu, Y Ma, L Chen, et al. 2025. Striking distance characteristics of lightning flashes striking at and below the top of the Canton Tower. Geophys Res Lett, 52, e2025GL115339. doi:10.1029/2025GL115339.

Qie X, D Liu, F Li, Z Sun, L Wei, et al. 2025. Charge structure of an isolated thunderstorm on the Tibetan Plateau and the formation of bolt-from-the-blue lightning. Chinese Science Bulletin, 70(7), 944-954. doi:10.1360/TB-2024-1144. (in Chinese)

Rafiuddin M, N Akter, A Dewan, M S G Adnan, R L Holle. 2025. Pre-monsoon lightning in Bangladesh: Separating most from least active days with thermodynamic and synoptic composites. Atmos Res, 325, 108261. doi:10.1016/j.atmosres.2025.108261.

Ringhausen J, A Alford, N Brauer, K Calhoun, V Chmielewski, S Waugh. 2025. Measurements from inside hurricane Ian using a mobile instrumentation network. Bull Am Meteorol Soc, doi: 10.1175/BAMS-D-23-0319.1.

Rycroft, M J. 2025. Some recent key aspects of the DC global electric circuit. Atmosphere, 16, 348. doi:10.3390/atmos16030348.

Samuel T O, J A Bolarinwa, O O Ayomide. 2025. Spatial structure, distribution, and fractal analysis of lightning waiting times in three global hotspots. J Atmos Sol-Terr Phy, 270, 106489. doi:10.1016/j.jastp.2025.106489.

Schatz S, S Pack, H Kohlmann, H Pichler, L Schwalt, et al. 2025. Enhanced short-term prediction of first cloud-to-ground lightning strikes in convective season thunderstorms. Electr Pow Syst Res, 247, 111810. doi:10.1016/j.epsr.2025.111810.

Shao X-M, D P Jensen, C Ho, M P Caffrey, E Y Raby, et al. 2025. 3D Radio frequency mapping and polarization observations show lightning flashes were ignited by cosmic-ray showers. J Geophys Res Atmos, 130, e2024JD042549. doi:10.1029/2024JD042549.

Shmuel A, T Lazebnik, O Glickman, O. et al. 2025. Global lightning-ignited wildfires prediction and climate change projections based on explainable machine learning models. Sci Rep, 15, 7898. doi:10.1038/s41598-025-92171-w.

Singh R, V Singh, A S Gautam, et al. 2025. Temporal and spatial variations in lightning activity and meteorological parameters across the Indian Himalayan region and Indo-Gangetic Plains. Asia-Pac J Atmos Sci, 61, 8. doi:10.1007/s13143-025-00391-x.

Slyunyaev N N, F G Sarafanov, N V Ilin, E A Mareev, E M Volodin, et al. 2025. The seasonal variation of the direct current global electric circuit: 1. A new analysis based on long-term measurements in Antarctica. J Geophys Res Atmos, 130, e2024JD042633. doi:10.1029/2024JD042633.

Slyunyaev N N, F G Sarafanov, N V Ilin, E A Mareev, E M Volodin, et al. 2025. The seasonal variation of the direct current global electric circuit: 2. Further analysis based on

simulations. J Geophys Res Atmos, 130, e2024JD042634. doi:10.1029/2024JD042634.

Smirnov S, S Pulinets, V Bychkov. 2024. Some effects of the shiveluch volcano eruption of the 10 April 2023 on atmospheric electricity and the ionosphere. Atmosphere, 15, 1467. doi:10.3390/atmos15121467.

Sobash R A, D A Ahijevych. 2025. Evaluating machine learning–based probabilistic lightning forecasts using the HRRR: A comparison to three forecast baselines. Weather Forecast, 40. doi:10.1175/WAF-D-24-0140.1.

Stucke I, D Morgenstern, G Diendorfer, G J Mayr, H Pichler, et al. 2025. Spatio-seasonal risk assessment of upward lightning at tall objects using meteorological reanalysis data. Earth Space Sci, 12, e2024EA003706. doi:10.1029/2024EA003706.

Syssoev A A, D I Iudin, F D Iudin, A A Emelyanov, I Y Zhavoronkov, et al. 2025. Numerical simulation of a lightning seed formation in a thundercloud. Atmos Res, 322, 108135. doi:10.1016/j.atmosres.2025.108135.

Tian C, X Wu, S Qiu, Y Li, L Shi. 2025. A graph neural network based workflow for real-time lightning location with continuous waveforms. J Geophys Res Atmos, 130, e2024JD042426. doi.org/10.1029/2024JD042426.

Trinh T N G, O Scholten, R van Loon, B M Hare, J D Assink, et al. 2025. Thunderstorm charge distribution determination using cosmic rays induced air showers and lightning imaging at LOFAR. Geophys Res Lett, 52, e2025GL115586. doi:10.1029/2025GL115586.

Unfer G R, L A T Machado, R I Albrecht, M A Cecchini, H Harder, et al. 2025. Decoding the relationship between cloud electrification, downdrafts, and surface ozone in the Amazon Basin. J Geophys Res Atmos, 130, e2024JD042158. doi.org/10.1029/2024JD042158.

Veloria A, Y Wada, H Hirose, D Kitahara, S Hayashi, et al. 2025. Introduction of lightning into the GSMaP rainfall measurements through optimized power-law model. J Atmos Oceanic Technol, 42, doi:10.1175/JTECH-D-24-0040.1.

Verjans V, C L E Franzke. 2025. Development of a data-driven lightning scheme for implementation in global climate models. J Adv Model Earth Syst, 17, e2024MS004464. doi:10.1029/2024MS004464.

Villamil S N, D Mestriner. 2025. Lightning-induced voltage on overhead conductors in urban areas: A study on how the air gap between buildings affects the shielding effect. Electr Pow Syst Res, 247, 111795. doi:10.1016/j.epsr.2025.111795.

Virts K S, W J Koshak. 2025. Bayesian analysis of the detection performance of the Geostationary Lightning Mappers. J Atmos Oceanic Technol, doi:10.1175/JTECH-D-24-0130.1.

Wang C, J Xia, R Jiang, Y Wu, H Shi, et al. 2025a. Deep learning-based lightning

nowcasting with embedded attention mechanisms. Chinese Journal of Atmospheric Sciences (in press).

Wang C, R Jiang, J Xia, Y Wu, H Shi, et al. 2025b. Infrared brightness temperature-based indicators for identifying thunderstorm clouds: Insights from FY-4A satellite observations. Atmospheric and Oceanic Science Letters (in press).

Wang C, X Zhang, H Yang, et al. 2025. Application research of convolutional neural network and its optimization in lightning electric field waveform recognition. Sci Rep, 15, 1883. doi:10.1038/s41598-025-85473-6.

Wang H, Y Tan, Z Shi, T Zheng. 2025. Effects of aerosols on diurnal variation of lightning activity in the Sichuan Basin, China. Atmos Res, 107943. doi: 10.1016/j.atmosres.2025.107943.

Wang X, B Wang, W Lyu, L Yu, L Hua, et al. 2025. Spatio-temporal evolution characteristics of optical radiation for tall-object lightning return stroke channels. Atmos Res, 325, 108240. doi:org/10.1016/j.atmosres.2025.108240.

Wang Y, B Cao, Y Fan, X Li, Y Zhang, et al. 2025. Relationship between X-rays and the propagation speed of downward negative leaders in rocket-triggered lightning. J Geophys Res Atmos, 130, e2024JD042818.

Wang Y, Y Zhao. 2025. A numerical study on the impacts of lightning data assimilation upon the simulation of a double rainband in Fujian, China. Atmos Res, 323, 108164. doi:10.1016/j.atmosres.2025.108164.

Wu B, Q Qi, W Lyu, Y Ma, F Lyu, et al. 2025. Effects of M-components on needle activity in positive cloud-to-ground lightning flashes. J Geophys Res Atmos, 130, e2024JD041797. doi:10.1029/2024JD041797.

Wu T, D M Smith, Y Wada, K Nakazawa, M Oguchi, et al. 2025. Energetic compact strokes as the major source of downward terrestrial gamma-ray flashes in winter thunderstorms. Geophys Res Lett, 52, e2024GL113194. doi:10.1029/2024GL113194.

Yamanaka A, K Ishimoto. 2025. Application of an integral-based solution of the field-to-line coupling formula to direct lightning surge analysis of distribution lines. IEEJ Trans Elec Electron Eng, doi:10.1002/tee.70049.

Yan X, S Chen, M Ding, C Chen, Y Zhang, et al. 2025. Surge impact characteristics of low-voltage overhead lines caused by natural lightning. IEEJ Trans Elec Electron Eng, doi:10.1002/tee.70010.

Yang Q, D Wang, J Yang, H Liu, T Wu, N Takagi. 2025. Initiation process of a winter cloud-to-ground lightning flash. J Geophys Res Atmos, 130, e2024JD041672. doi:10.1029/2024JD041672.

Yang Q, D Wang, J Yang, T Wu. 2025. Observation of the first stepping process of three winter lightning discharges. Geophys Res Lett, 52, e2024GL111468. doi:10.1029/2024GL111468.

Yang Q, D Wang, T Wu. 2025. Preliminary breakdown process of winter positive cloud-to-ground lightning and its relation to the following first return stroke. J Geophys Res Atmos, 130, e2024JD041496. doi:10.1029/2024JD041496.

Yu R, M Du, D Zheng, J Wang. 2025. Analysis of anomalous cloud-to-ground lightning in a Wuhan tornadic supercell on 14 May 2021. Atmos Res, 320, 108056. doi:10.1016/j.atmosres.2025.108056.

Yu X, D Zheng, Y Zhang, W Yao, W Zhang. 2025. Higher proportion of high-energy lightning strokes in global high-altitude areas. Geophys Res Lett, 52, e2024GL112407. doi:10.1029/2024GL112407.

Zhang Z, T Deng, X Zhang, H Huang, G He, et al. 2025. The influence of aerosols on lightning activity in the Pearl River Delta of China. Atmos Res, 321, 108066. doi:10.1016/j.atmosres.2025.108066.

Zheng T, Y Tan, F Lyu, W Lyu. 2025. Numerical simulation study of the evolution of lightning channel decay and reactivation processes. J Geophys Res Atmos, 130, e2024JD042844. doi:10.1029/2024JD042844.

Zhu B, B Lin, B Liu, H Liu. 2025. Analysis of temporal and spatial distribution of CG lightning activity and its relationship with terrain features around Jiuxianshan mountain. J Atmos Sol-Terr Phy, 273, 106546. doi:10.1016/j.jastp.2025.106546.

ATMOSPHERIC ELECTRICITY

NEWSLETTER

Vol.36 No.1 2025 May

Edited by: Wenjuan Zhang (CAMS) and Haiyang Gao (NUIST)

REMINDER

Newsletter on Atmospheric Electricity presents twice a year (May and November) to the members of our community with the following information:

- ✧ announcements concerning people from atmospheric electricity community, especially awards, new books...,
- ✧ announcements about conferences, meetings, symposia, workshops in our field of interest,
- ✧ brief synthetic reports about the research activities conducted by the various organizations working in atmospheric electricity throughout the world, and presented by the groups where this research is performed, and
- ✧ a list of recent publications. In this last item will be listed the references of the papers published in our field of interest during the past six months by the research groups, or to be published very soon, that wish to release this information, but we do not include the contributions in the proceedings of the Conferences.

No publication of scientific paper is done in this Newsletter. We urge all the groups interested to submit a short text (one page maximum with photos eventually) on their research, their results or their projects, along with a list of references of their papers published during the past six months. This list will appear in the last item. Any information about meetings, conferences or others which we would not be aware of will be welcome.

Call for contributions to the newsletter

All issues of this newsletter are open for general contributions. If you would like to contribute any science highlight or workshop report, please contact Weitao Lyu (weitao.lyu@gmail.com) preferably by e-mail as an attached word document.

The deadline for **2025 winter issue** of the newsletter is **Nov 15, 2025**.

PRESIDENT
Xiushu Qie
Chinese Academy of Sciences
E-mail: qiex@mail.iap.ac.cn

SECRETARY
Weitao Lyu
Chinese Academy of Meteorological Sciences
E-mail: weitao.lyu@gmail.com

ICAE

IAMAS IUGG